bioRxiv preprint doi: https://doi.org/10.1101/2023.01.24.525215; this version posted January 24, 2023. The copyright holder for this preprint (which was not certified by peer review) is the author/funder. All rights reserved. No reuse allowed without permission.

CAM5, WRKY53, and TGA5 regulate defense gene expression mediated by the volatile organic compound ethyl vinyl ketone

Junqing Gong[1†], Zhujuan Guo[1†], Zhaoyuan Wang[1†], Lijuan Yao[1], Chuanfang Zhao[2], Sheng Lin[2], Songling Ma[2], Yingbai Shen[1*]

1 National Engineering Research Center of Tree breeding and Ecological restoration, College of Biological Sciences and Technology, Beijing Forestry University, No. 35, Qinghua East Road, Beijing 100083, P. R. China

Junqing Gong (gongjunqing2022@126.com); Zhujuan Guo (gzj2190073@163.com); Zhaoyuan Wang (Alice0521@bjfu.edu.cn); Lijuan Yao (ylj52386@163.com)

2 Beijing Jingtai Technology Co., Ltd., Beijing 100083, P. R. China

Chuanfang Zhao (chuanfang.zhao@xtalpi.com); Sheng Lin (sheng.lin@xtalpi.com); Songling Ma (songling.ma@xtalpi.com)

*Correspondence: ybshen@bjfu.edu.cn

†These authors contributed equally to this work.

Abstract

Plants produce ethyl vinyl ketone (evk) in response to biotic stress, but the evk's identification and downstream defense response remain unclear. In this paper, it is predicted by docking for the first time that evk can be recognized by RBOH protein and assist the electron transfer of RBOHD/RBOHF by binding to its FAD or NADPH binding site. Here, we show that evk treatment increased H_2O_2 and intracellular calcium concentrations in *Arabidopsis thaliana* mesophyll cells, as observed by confocal laser scanning microscopy and non-invasive micro-test technology, and that H_2O_2 signaling functioned upstream of Ca^{2+} signaling. Yeast two-hybrid, firefly luciferase complementation imaging, and *in vitro* pull-down assays demonstrated that the ACA8 (AUTOINHIBITED Ca^{2+}-ATPASE, ISOFORM 8)–CML8 (CALMODULIN-LIKE 8) interaction promoted Ca^{2+} efflux to return Ca^{2+} levels to the resting state. Evk treatment led to the antagonism of salicylic acid (SA) and jasmonic acid (JA). CALMODULIN 5 (CAM5) positively regulates *WRKY53* expression, and CAM5 and WRKY53 positively regulate SA-related gene expression. These proteins physically interact and form a complex that is unlocked by Ca^{2+} to release WRKY53. An electrophoretic mobility shift assay and dual-luciferase reporter assay demonstrated that WRKY53 and TGA5 cooperate to enhance the expression of the defense gene *PATHOGENESIS-REALTED 1* (*PR1*) and that WRKY53 enhances the binding of TGA5 to the *PR1* promoter. This paper proposes a framework that evk, as a RES substance, can achieve plant's 'REScue' through complete defense response.

Keywords: Arabidopsis; volatiles; ethyl vinyl ketone; molecular docking; pathogens; JA; SA

Introduction

The classical ligand receptor reversible perception mechanism usually includes the following steps: Biological production of specific hormones; hormones are released and transported to specific locations; hormones bind through transmembrane or soluble receptor proteins; it transmits perceived hormone signals through signal transduction process and mediates cell reaction;

bioRxiv preprint doi: https://doi.org/10.1101/2023.01.24.525215; this version posted January 24, 2023. The copyright holder for this preprint (which was not certified by peer review) is the author/funder. All rights reserved. No reuse allowed without permission.

hormone cycle is used for the next round of signal perception and transmission, or hormone decomposition to prevent hormone signal transmission[1]. In the past decades, many previous studies have revealed how plants perceive and transduce JA to confer plant defense. It is known that JA is sensed by COI1 receptor and induces JAZ inhibitor degradation[2], leading to rapid activation of JA response genes necessary for JA regulated plant response. Defensive response refers to a series of specific internal metabolic changes and external structural changes of plants to improve their survival ability against insect and pathogen invasion, including: external stimulus recognition, stimulus signal transduction, expression and regulation of defense genes, synthesis and accumulation of bioactive substances, defense effect realization and other biological processes. Evk is one of the plant volatiles. It is not clear how plants recognize evk to mediate the signal transduction and cause plant defense process. The event is still unknown.

Volatile organic compounds can be released from plants in response to insect feeding, mechanical injury, or infection. Plant volatiles often play major roles in regulating insect and microbe feeding on plants[3]. Volatiles containing α,β-unsaturated carbonyls are known as reactive electrophilic substances (RESs)[4,5]. Cells can benefit from lipid peroxidation and RES production while under stress. For instance, RESs modulate gene expression via a class II TGA transcription factor module and unknown signaling pathways. RES signaling promotes cell "REScue" by activating genes encoding detoxification enzymes, cell cycle regulators, and chaperones. Most biological activities of oxygenated lipid (oxylipin) in plants are mediated by either jasmonate (JA) perception or RES signaling networks[6]. Notably, numerous secondary compounds, including many phenolics and terpenes, exhibit electrophilic properties (such as α,β-unsaturated carbonyl groups), suggesting that such lipid-derived molecules may have been among the earliest direct defense chemicals to emerge[7]. Other secondary compounds exhibit behaviors that strongly suggest unique, defense-related functions, although their roles are unknown. One of these compounds is malondialdehyde (MDA), which has a variety of variants, each with unique characteristics[8]. While many other minor RESs are volatile and can be released after an attack, the protonated form of MDA is likely too reactive to escape from plants as a volatile. MDA enhanced endogenous JA and salicylic acid (SA) in Arabidopsis after *Botrytis cinerea* infection[9]. (E)-2-hexenal is an electrophilic compound that is synthesized and released quickly during bacterial infection or insect feeding[10,11,12]. Although methyl vinyl ketone is toxic to cells at high concentrations[13,14], such substances might activate the expression of genes such as *HEAT SHOCK PROTEIN 101* (*HSP101*) in isoprene-producing plants. Furthermore, 12-oxo-phytodienoic acid (OPDA), an electrophilic chemical, can be employed as a signaling molecule to increase the expression of a wide range of genes other than JA-related genes[15,16,17]. Mattick and Hand were the first to discover ethyl vinyl ketone (evk) in soybean (*Glycine max* (L.) *Merr.*) homogenates[18].

Evk is a small, volatile chemical molecule with an α, β-unsaturated carbonyl structure that activates the expression of defense genes in Arabidopsis (*Arabidopsis thaliana*). Evk was released as a pest-induced plant volatile when cabbage butterfly (*Pieris rapae*) was fed to Arabidopsis[19]. Soybean produced evk in a 13-HOPT-dependent manner when LIPOXYGENASE (LOX) activity was inhibited[20]. When damaged by freeze-thaw and oxygen stress, soybean leaves emit a substantial amount of evk[21]. The occurrence of floral end rot was reduced by increasing the evk content of tomatoes (*Solanum lycopersicum*) by treating the plants with selenium during the green blossom stage[22]. We previously demonstrated that evk-induced stomatal closure requires MULTIDRUG RESISTANCE-ASSOCIATED PROTEIN 4 (MRP4)-dependent extracellular ATP

bioRxiv preprint doi: https://doi.org/10.1101/2023.01.24.525215; this version posted January 24, 2023. The copyright holder for this preprint (which was not certified by peer review) is the author/funder. All rights reserved. No reuse allowed without permission.

accumulation and subsequent H_2O_2 accumulation to regulate K^+ efflux[23]. Evk is involved in many biological processes, but whether it activates defense genes (e.g., *PLANT DEFENSIN 1.2* [*PDF1.2*] and *PATHOGENESIS-RELATED 1* [*PR1*]) remains unknown.

Ca^{2+} acts as a crucial early signal during plant defense responses. When plants detect external signs of pathogen attack, such as oral elicitors from insects or bacterial flagella, Ca^{2+} from intracellular calcium stores (in the vacuole, Golgi apparatus, or endoplasmic reticulum [ER]) or extracellular calcium stores (in the interstitial spaces between the cell wall and plasmids) immediately flow into the cytoplasm[24,25]. The Ca^{2+}/proton antiporter system and Ca^{2+}-ATPases are responsible for returning Ca^{2+} to the calcium reserves once it has fulfilled its function as a second messenger[26].

Two mechanisms in plants require both Ca^{2+} and H_2O_2: Ca^{2+}-induced ROS generation and ROS-induced Ca^{2+} release. Co-expressing *AtSRC2* (*SOYBEAN GENE REGULATED BY COLD 2*) and *RBOHF* in human embryonic kidney (HEK293) cells enhanced the production of ROS mediated by a Ca^{2+}-dependent ROS burst[27]. Under salt stress, Ca^{2+} and ROS (whose production relies on AtRBOHD) concurrently undergo long-distance transmission[28]. When Ca^{2+} binds to the NADPH oxidase EF-hand domain, the chiral structure of the EF-hand undergoes a conformational change that is required for RBOHD activation. ROS directly activate or inhibit the activity of Ca^{2+} channels or pumps that control Ca^{2+} concentrations, representing the primary source of ROS-induced Ca^{2+} release[29].

The w-box sequence is frequently present in the upstream regulatory regions of genes activated by SA, as well as genes related to plant disease resistance, the damage response, and senescence. Various biological and abiotic stress reactions are tightly associated with WRKY transcription factors[30-35]. WRKY53 positively regulates resistance to *Pseudomonas syringae*[36]. WRKY53 and EPITHIOSPECIFIER PROTEIN (ESR) mediate the antagonistic relationship between pathogen resistance and aging[37], which likely involves the JA/SA balance. EMSAs (electrophoretic mobility shift assays) demonstrated that the DNA binding ability of WRKY53 is inhibited by ESR in the presence of WRKY53 *in vitro*[38,39]. WRKY53 positively regulates stomatal opening and boosts starch metabolism by lowering the amount of H_2O_2 in guard cells and directly binding to the *QUA-QUINE STARCH* (*QQS*) promoter[40]. In Arabidopsis, the presence of w-boxes in the *ALLENE OXIDE SYNTHASE* (*AOS*) promoter is required for binding by JASMONATE-ASSOCIATED VQ MOTIF GENE 1 (JAV1) and WRKY51[41].

Calmodulin (CaM) responds to a range of stress and plant hormonal cues, including H_2O_2 and SA, by selectively binding to the CGCG-box sequences in the promoters of its target genes and activating their transcription[42,43]. Ca^{2+}/CaM-mediated regulatory signals have long been known to play essential roles in maintaining H_2O_2 homeostasis, plant growth and development, plant-microbial symbiosis, immunological response, and freezing tolerance. A fascinating question about the underlying cell signal transduction network is how plants begin with the release of the simple second messenger intracellular Ca^{2+} ions in response to a variety of external stimuli, form Ca^{2+}/CaM signals by binding to CaM, and interpret these signals into various physiological response processes accurately and efficiently[44,45].

Special electrophile structures can also covalently modify proteins, including cyclopentenone, an important regulator of plant development and responses to biotic and abiotic stress[46,47]. Its α, β-unsaturated carbonyl structure confers chemical reactivity to mercaptan, which is essential for protein activity[4,6,48]. TGACG MOTIF-BINDING FACTOR 2 (TGA2) enhances

bioRxiv preprint doi: https://doi.org/10.1101/2023.01.24.525215; this version posted January 24, 2023. The copyright holder for this preprint (which was not certified by peer review) is the author/funder. All rights reserved. No reuse allowed without permission.

cyclopentenone-induced changes in gene expression. TGA2 activity is regulated in part by RES-dependent post-translational modification. TGA2 is covalently modified by Prostaglandin A1 (PGA1)-biotin (a RES not found in plants) and OPDA (an important plant RES). Extreme temperature and pH conditions can make covalently modified TGA2 vulnerable[49]. The carbonyl cyclopentenone ring in PGA1 may react with protein thiol (Cys) and/or primary amine (Lys, Arg)[50]. The primary production of conjugates relies on mercaptan modification, which occurs when PGA1-biotin modifies TGA2 at Cys-186 by Michael addition. A deletion mutant of a type II TGA transcription factor (*tga2*, *tga5*, or *tga6*) is unable to trigger PPA1 and OPDA production. When TGA2,5,6 mutations occur, the up regulation of α,β-unsaturated carbonyl structure-mediated gene decreases by 60%. A putative binding site (TGACG) for basic leucine zipper (bZIP) transcription factors of the TGA family with a TGA motif is present in the promoters of approximately 50% of cyclopentenone-induced genes[50]. These findings suggest that TGA transcription factors might function in response to RES[51].

TGA-binding sites are found in the promoters of several genes and can react to a variety of signals during responses to pathogens, trauma, and xenobiotic stress[52-54]. Most JA-induced genes are not TGA dependent, while the majority of TGA-dependent detoxifying genes are not induced by JA[55]. In various yeast two-hybrid screening experiments, NPR1 was shown to interact with the TGA subclass of bZIP transcription factors[56,57]. These TGA transcription factors can bind to the as-1 element in the *PR1* promoter, which is required for the response of this gene to SA. The TGA2-NPR1 complex is better able to form in the presence of SA. Active NPR1 increases the binding of TGAs to the as-1 sequence in the *PR1* promoter, thereby increasing its expression[58].

TGA3 and WRKY53 physically interact and regulate the activity of the *Cestrum yellow leaf curling virus* (CmYLCV) promoter. The two distinct types of TGA and WRKY transcription factors are known to interact[59], but the nature if this interaction is not well understood. To regulate the expression of *PR1* in response to SA induction, the transcription factors TGA2 and AtWRKY50 bind to as-1 and the w-box in the *PR1* promoter, respectively (at an interval of 8 bp)[60]. In the presence of NPR1, the transcription of the CmYLCV promoter is regulated by SA only in the presence of TGA3 and WRKY53. SA-mediated *PR1* transcription in Arabidopsis is significantly affected by the TGA/NPR1 interaction[61,62].

Here, we show that evk can be recognized by RBOH protein and evk treatment increases intracellular H_2O_2 and Ca^{2+} concentrations in leaves, as revealed using non-invasive micro-test technology (NMT) and confocal laser scanning microscopy. Together, CML8 and ACA8 transport Ca^{2+} out of the cytoplasm and lower cytoplasmic Ca^{2+} concentrations. Additionally, RBOHD and RBOHF influence the ROS burst as well as the rise in intracellular Ca^{2+} concentrations and the outflow of calcium ions. Therefore, evk functions as a signal that causes variation in Ca^{2+} and H_2O_2 concentrations in Arabidopsis leaves. We performed EMSAs and yeast two-hybrid, firefly luciferase complementation imaging, *in vitro* pull-down, and luciferase activity assays to explore how CAM5 and WRKY53 govern *PR1* and *PDF1.2* expression. High Ca^{2+} concentrations caused the CAM5-WRKY53 complex to disassemble, which released WRKY53. The released WRKY53 can interact with TGA5 in the nucleus, thereby increasing its ability to associate with the *PR1* promoter. WRKY53 binds to the *PDF1.2* promoter via its w-box, but the released WRKY53 can prevent TGA5 from binding to as-1 in the *PDF1.2* promoter. We also performed a dual-luciferase reporter assay to explore how both WRKY53 and TGA5 increase the transcription of *PR1*. WRKY53 and TGA5 more effectively triggered the expression of *PR1* together than separately.

bioRxiv preprint doi: https://doi.org/10.1101/2023.01.24.525215; this version posted January 24, 2023. The copyright holder for this preprint (which was not certified by peer review) is the author/funder. All rights reserved. No reuse allowed without permission.

PDF1.2 was downregulated by WRKY53 but upregulated by TGA5.

Materials and methods

Computational detials

Our experimental results indicated that the ethyl vinyl ketone (evk)-mediated ROS burst is dependent on RBOHD and RBOHF, but how evk binds with RBOHD/RBOHF is still unknown. To explore the mode of evk on RBOHD or RBOHF, their interactions were mimicked with Molecular Operating Environment (MOE) 2020.09 software (Chemical Computing Group Inc., Montreal, Canada).

Homology modeling of RBOHD and RBOHF

The crystal structure of AtRBOHD and AtRBOHF had not been reported, therefore 3D structures of them were built with homology modeling firstly. Homology modeling of AtRBOHD and AtRBOHF were executed with SwissModel, which is a fully automated protein homology modeling server (https://swissmodel.expasy.org/). The sequences of AtRBOHD and AtRBOHF were downloaded from UniProt website (Uniprot code: Q9FIJ0 and O48538). The 3D structure of AtRBOHD was built, with the QMEANDisCo Global is 0.60, GMQE is 0.48, and 30.01% sequence identity with human DUOX1-DUOXA1. And the 3D structure of AtRBOHF was built with the QMEANDisCo Global is 0.59, GMQE is 0.47, and 28.38% sequence identity with human DUOX1-DUOXA1.

Binding site exploration and docking simulations

The possible binding sites of AtRBOHD and AtRBOHF were explored with Site Finder module in the MOE software. The top two recommended binding sites were used as binding sites of AtRBOHD and AtRBOHF, corresponding to the FAD and NADPH binding site of the highly homologous human DUOX1-DUOXA1 (PDB code, 7D3F). Docking were carried out with default parameters (Placement setting as Triangle Matcher, Refinement setting as Rigid Receptor) to explore the binding interactions between evk and AtRBOHD and AtRBOHF.

Plant materials and culture conditions

Wild-type (WT) Arabidopsis accession Col-0, the *cam5* mutant SALK_007371 (At2g27030), and the *wrky53* mutant SALK_034157 (At4g23810) were used as plant materials. The *wrky53* mutant was kindly provided by Prof. Diqiu Yu (Xishuangbanna Tropical Botanical Garden, Chinese Academy of Sciences, China). The *cml8-1* mutant SALK_022524C (At4g14640) and the *cml8-2* mutant SALK_114570C (At4g14640) were used as plant materials. Seeds were stratified at 4°C for 2 days in the dark. After stratification, seeds were surface-sterilized for 4 min in 75% (v/v) ethanol, washed four times in sterile water, sown on autoclaved soil mixture, and placed in an incubator (Percival model: I-36vl). Plants were grown on soil at 21–23°C and 70% relative humidity with a light intensity of 80–110 μmol m^{-2} s^{-1} under long-day (16 h light/8 h dark) conditions. The plants used for insect inoculation were grown for 4 weeks, and the seedlings used in all other experiments were grown for 2 weeks prior to treatment.

Evk treatment

Arabidopsis plants were treated with evk (≥97%, purchased from Sigma) via fumigation in

bioRxiv preprint doi: https://doi.org/10.1101/2023.01.24.525215; this version posted January 24, 2023. The copyright holder for this preprint (which was not certified by peer review) is the author/funder. All rights reserved. No reuse allowed without permission.

glass bell jars (height: 12.5 cm; diameter: 15 cm). Cotton balls 1 cm in diameter were soaked in evk dissolved in ethanol (evk at a final concentration of 5 μM) and hung in the bell jars; cotton balls soaked in the same volume of ethanol were used as control. After adding the cotton balls, the bell jars were immediately sealed with Vaseline petroleum jelly.

Ca^{2+} flux measurements in mesophyll cells

Ca^{2+} flux in mesophyll cells was measured using the non-invasive micro-test technique (NMT, BIO-001A, Younger USA). Before the test, small cuts were made in the leaves of 3-week-old Arabidopsis plants. The leaves were soaked in test solution (0.1 mM KCl, 0.1 mM $CaCl_2$, 0.1 mM $MgCl_2$, 0.5 mM NaCl, 0.3 mM MES, 0.2 mM Na_2SO_4, pH 6.0) for approximately 30 min. Silanized glass micropipettes (2- to 4-μm aperture) were filled with electrolyte solution (100 mM $CaCl_2$) and front-filled with a selective liquid ion exchange (LIX) cocktail to approximately 10 μm. The glass micropipettes were connected to the NMT system with a silver chloride wire, and electrodes with Nernstian slopes of 28 ± 5 mV log^{-1} were used.

The Ca^{2+} concentrations in mesophyll cells were measured near the cells and 30 μm away from the cells at 0.2 Hz. Each leaf was tested for 2 min before evk treatment (pre-evk treatment; pre). After evk was quickly added to the test solution to a final concentration of 10 μM, data were collected for approximately 2.5 min as the evk response peak (peak) group. Data were then collected from the post-evk response (post) group to indicate the end of the reaction. The final flux values are reported as the mean of eight individual plants per treatment. The Ca^{2+} flux was calculated as:

$$J = -D\frac{\Delta C}{\Delta X},$$

where J is the flux of Ca^{2+} (pmol cm^{-2} s^{-1}), D is the diffusion coefficient (0.79 ×10^{-5} cm^{-2} s^{-1}), ΔC is the difference between the concentrations near and far from the cells, and ΔX is 30 μm. Each group contained six to eight replicates.

Ca^{2+} fluorescence measurements in mesophyll cells

Prior to treatment with Fluo3-AM (10 μM), Arabidopsis leaves were soaked in test solution (the same solution used for the Ca^{2+} flux experiment). The leaves were then soaked in Fluo3-AM solution to label Ca^{2+} ions for 1 h in the dark in an incubator. The leaves were washed and placed in fresh test solution. Ca^{2+} fluorescence was detected with a confocal laser scanning microscope (Leica TCS SP8). The excitation wavelength was 488 nm, and the emission wavelength was 530 nm. Before adding evk (0 min), the basal level of Ca^{2+} fluorescence in mesophyll cells was measured. Following the addition of evk, fluorescence was measured every 30 s for 150 s. Each group contained 20–40 cells.

The increase in Ca^{2+} fluorescence was calculated as (X − a) / a * 100%, where X is the fluorescence of evk-treated samples and a is fluorescence at 0 s. The value for each group was calculated separately.

H_2O_2 fluorescence measurements in mesophyll cells

To observe transient evk responses, H2DCF-DA was used to measure changes in H_2O_2 levels in Arabidopsis mesophyll cells. Following incubation in the test solution, the leaves were incubated in 50 μM H2DCF-DA for 12 min at 25℃ in the dark. Confocal laser scanning

bioRxiv preprint doi: https://doi.org/10.1101/2023.01.24.525215; this version posted January 24, 2023. The copyright holder for this preprint (which was not certified by peer review) is the author/funder. All rights reserved. No reuse allowed without permission.

253 microscopy (Leica TCS SP8, Leica Microsystems, Wetzlar, Germany) was used to detect H_2O_2
254 fluorescence with excitation at 490 nm and emission at 530 nm. H_2O_2 fluorescence measurements
255 were obtained at 0 min (before the addition of evk) and every 3 min for 12 min. Each group
256 contained 30 cells.

257 ## RT-qPCR

258 For quantitative RT-PCR, total RNA was extracted from the samples using an RNA extraction kit,
259 and first-strand cDNA was generated using a reverse transcriptase kit (Takara). qPCR was
260 performed in a 7500 fast real-time PCR system (Applied Biosystems, Foster City, California, USA)
261 using a Power SYBR Green PCR Master Mix kit (Applied Biosystems, Foster City, California,
262 USA), and the $2^{-\Delta\Delta Ct}$ method was used to calculate relative gene expression levels. The expression
263 levels of several important genes in the JA and SA were measured, See Supplementary 1 for
264 primer information.
265

266 ## Measuring JA/SA levels in leaves

267 JA and SA levels were measured in Arabidopsis leaves in six experimental groups (WT
268 control group and WT evk group), and analysis was performed on an Agilent 1290 system with
269 AB SCIEX-6500Qtrap. Each group had three biological replicates.
270

271 ## Arabidopsis protoplast isolation and transformation

272 Arabidopsis protoplasts were isolated from leaf tissues of 14-day-old seedlings. Cut leaves
273 into 0.5-1 mm thin strips, and soak them in 0.5 M mannitol solution for 30 min. Take out the sliver
274 and put it into the enzymolysis solution (0.4 M mannitol, 20 mM KCl, 20 mM MES, 1.5%
275 cellulase R-10, 0.4% macrozyme, 10 mM $CaCl_2$) to avoid light, 23 ℃, 50 rpm, and enzymolysis
276 on the shaking table for 3 hours. When the hydrolysate turns green, gently shake the culture dish
277 to release protoplasts. Use a 40 μm cell sieve to filter the protoplasts into a centrifuge tube. Add an
278 equal volume of W5 solution (2mM MES pH7.5, 154mM NaCl, 125mM $CaCl_2$, 5mM KCl).
279 Centrifuge at 4 ℃ for 2 min at 100 × g. Add an equal volume of W5 solution. Repeat the washing
280 once. Shake the centrifuged protoplasts gently and suspend them on ice for 30 min. Add an
281 appropriate amount of precooled MMG solution (4 mM MES pH 5.7, 0.4 M mannitol and 15 mM
282 $MgCl_2$) to wash the protoplast, centrifuge for 1min, discard the supernatant, add an appropriate
283 amount of MMG solution to suspend the protoplast, and transform PEG: the following steps are to
284 take 10 μg of plasmid at 23 ℃ and put it into a 1.5ml centrifuge tube, add 100 μl of protoplast
285 extract, and then add 110 μl of PEG conversion solution, mix it well, place it at 23 ℃ and
286 incubate it in dark for 30 min, and transform it, the transfection mixture was diluted with 400 μl
287 W5 solution to stop the transfection process followed by centrifugation at 100 × g for 1min at
288 room temperature, incubation overnight in the dark in a 23 ℃ growth chamber.

289 ## Dual-luciferase reporter assay

290 The *PR1* and *PDF1.2* promoters were cloned into pGreenII 0800-LUC and the *WRKY53*,
291 *CAM5*, and *TGA5* coding sequences were cloned into pGreenII 62-SK. The resulting plasmids
292 were transformed into Agrobacterium (*Agrobacterium tumefaciens*) strain GV3101 and used to

bioRxiv preprint doi: https://doi.org/10.1101/2023.01.24.525215; this version posted January 24, 2023. The copyright holder for this preprint (which was not certified by peer review) is the author/funder. All rights reserved. No reuse allowed without permission.

infiltrate *Nicotiana benthamiana* leaves. Luciferase activity in infiltrated *N. benthamiana* leaves was imaged using a molecular imaging system (LB983). Firefly luciferase (LUC) and Renilla luciferase (REN) activities were measured using a Dual Luciferase Reporter Gene Assay Kit with a GloMax 96 Luminometer.

Electrophoretic mobility shift assay (EMSA)

The w-boxes in *PR1*, *PDF1.2* promoter, and the as-1 element in the *PDF1.2* promoter were used to generate 3′-biotin-labeled probes. The CDS of CAM5 was cloned into pMAL-C2X with BamHI/SalI, the CDS of TGA5 was cloned into pMAL-C2X with BamHI/EcoRI, and the CDS of WRKY53 was cloned into MAL-C2X with BamHI/SalI. MBP, CAM5-MBP, TGA5-MBP, and WRKY53-MBP were transformed into *E. coli* Rosetta (DE3) cells for protein expression. MBP (as a control) was used in EMSAs with a LightShift Chemiluminescent EMSA Kit (Thermo Scientific) following the manufacturer's protocol. The probe sequences used in the EMSA were as Supplementary 2.

Firefly luciferase complementation imaging assay (LCI)

The *TGA5*, *CAM5*, and *CML8* coding sequences were cloned individually into the CLuc plasmid, and the *WRKY53* and *ACA8* coding sequences were cloned into the NLuc plasmid. The resulting plasmids were transformed into Agrobacterium strain GV3101. Luminescence signal from *Nicotiana tabacum* leaves infiltrated with the Agrobacterium cultures was imaged with a molecular imaging system (LB983, Berthold Technologies, Germany). Each leaf was divided into four quadrants prior to infiltration with the following combinations: *CLuc/NLuc*, *CAM5-CLuc/NLuc*, *CLuc/WRKY53-NLuc*, and *CAM5-CLuc/WRKY53-NLuc*; *CLuc/NLuc*, *CML8-CLuc/NLuc*, *CLuc/ACA8-NLuc*, and *CML8-CLuc/ACA8-NLuc*; or *CLuc/NLuc*, *TGA5-CLuc/NLuc*, *CLuc/WRKY53-NLuc*, and *TGA5-CLuc/WRKY53-NLuc*.

In vitro pull-down assay

The coding sequences for *TGA5*, *CML8*, and *CAM5* were cloned into pGEX-4T-1, and the *ACA8* (aa 1–180), and *WRKY53* coding sequences were cloned into pET28A. The resulting CAM5-GST, CML8-GST, *TGA5*-GST, ACA8-HIS, and WRKY53-HIS plasmids were transformed into *E. coli* Rosetta (DE3) cells for protein production. Recombinant protein-GST was used as bait. The binding of CAM5-GST to WRKY53-HIS, *TGA5*-GST to WRKY53-HIS, and CML8-HIS to ACA8-GST was detected by immunoblot analysis using anti-GST and anti-HIS antibodies.

Yeast two-hybrid assay

The coding sequences of *CML8* and *CAM5* were cloned into pGADT7, and the sequences encoding residues 1–217 of WRKY53 (WRKY53 [aa 1–217]) and residues 1–180 of ACA8 (ACA8 [aa 1–180]) were cloned into pGBKT7. The appropriate plasmid pairs CAM5-AD plus WRKY53 (1–217 aa)-BK and CML8-AD plus ACA8 (1–180 aa)-BK were co-transformed into competent yeast strain AH109 cells. The cells were grown on synthetic defined (SD) –Leu –Trp medium. After 4 days, growing colonies were transferred to SD medium –Ade –His –Leu –Trp for verification. Growing colonies on SD medium –Ade –His –Leu –Trp were transferred to SD

bioRxiv preprint doi: https://doi.org/10.1101/2023.01.24.525215; this version posted January 24, 2023. The copyright holder for this preprint (which was not certified by peer review) is the author/funder. All rights reserved. No reuse allowed without permission.

medium –Ade –His –Leu –Trp with X-α-gal. Cell growth on SD –Leu –Trp and SD –Ade –His –Leu –Trp and blue colonies on SD –Ade –His –Leu –Trp with X-α-gal indicate protein–protein interactions between the two proteins.

Bimolecular fluorescence complementation assay

TGA5 was cloned into the pSPYNE vector via BamHI/SalI, WRKY53 was cloned into the pSPYCE vector via BamHI/SalI, and the plasmids were transformed into Agrobacterium strain GV3101. Both constructs (DORN1-YNE and RBOHF-YCE) were transformed into *N. tabacum* leaves infected with Agrobacterium. YFP fluorescence was imaged with confocal laser scanning microscopy (Leica TCS SP8, Leica Microsystems, Wetzlar, Germany) at an excitation wavelength of 510 nm and an emission wavelength of 510–530 nm.

Statistical Analysis

Dunnett's C (variance not neat) at the level of $p < 0.05$ was significant. Error bars denote ± standard error of mean (SEM).

Results

The evk-mediated ROS burst is dependent on RBOHD and RBOHF

We performed confocal laser scanning microscopy to measure H_2O_2 contents in Arabidopsis mesophyll cells. After 15 min of evk treatment, fluorescence from oxidized 2′,7′-dichlorofluorescein (DCF, reflecting H_2O_2 contents) consistently increased in mesophyll cells compared to the control (Figure 1a). Indeed, compared to the control, the fluorescence intensity increased by 196.2% (after 3 min), 309.1% (6 min), 252.9% (9 min), and 175.0% (15 min), suggesting that evk might cause mesophyll cells to generate H_2O_2 on a continual basis. The temporary addition of evk considerably reduced the fluorescence intensity of H_2O_2 in the NADPH oxidase *rbohd rbohf* double mutant. These findings suggest that the evk-induced ROS burst is mediated by NADPH oxidase. The fluorescence intensity after evk treatment rose by 268.9% (3 min), 285.5% (6 min), 217.4% (9 min), and 199.8% (15 min) in wild-type plants pretreated with ruthenium red (a Ca^{2+} channel inhibitor that blocks the release of internal Ca^{2+}), values that were not significantly different from those of the WT+evk treatment group (Figure 1b). These results demonstrate that NADPHase is involved in the evk-induced ROS burst and that changes in calcium concentrations have no effect on the evk-induced H_2O_2 burst.

bioRxiv preprint doi: https://doi.org/10.1101/2023.01.24.525215; this version posted January 24, 2023. The copyright holder for this preprint (which was not certified by peer review) is the author/funder. All rights reserved. No reuse allowed without permission.

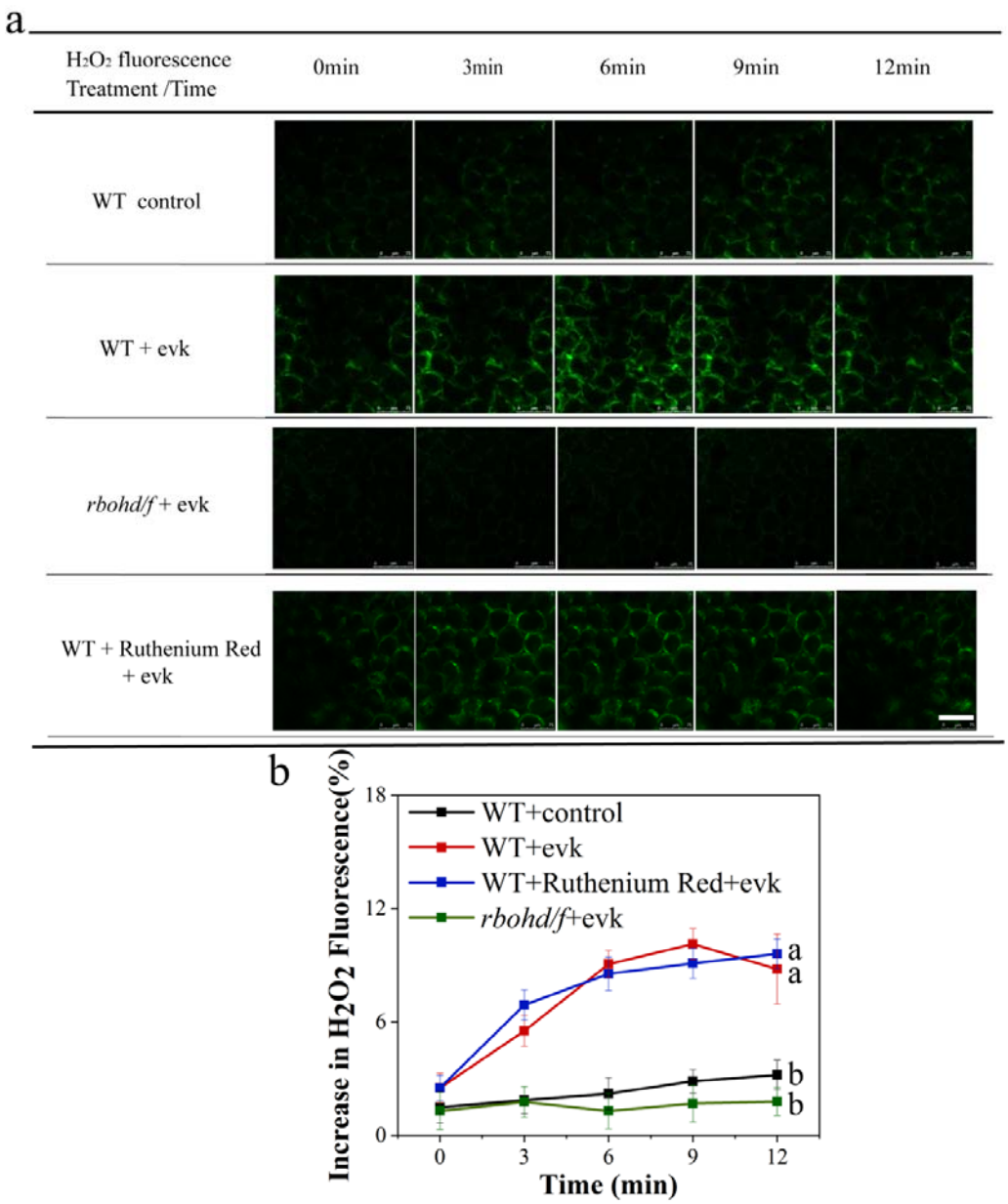

Figure 1. evk-induced increases in H_2O_2 levels depend on RBOHD, RBOHF but not on internal Ca^{2+} release channels in Arabidopsis mesophyll cells.

(a) ROS burst in response to evk treatment in the wild type (WT), *rbohd rbohf*, and WT pretreated with ruthenium red. The cells were washed to remove the 50 μM H_2DCF-DA test solution (0 min), evk was added, and the cells were photographed every 3 min. Scale bars, 75 μm. (b) H_2O_2 fluorescence over time in ruthenium red–treated and *rbohd rbohf* cells compared to the WT evk group. Analysis of changes in H_2O_2 fluorescence indicated that increases in H_2O_2 fluorescence were significantly suppressed in *rbohd rbohf* cells compared to the WT + evk-treated group but were unaffected in ruthenium red–treated cells. The seedlings plants were grown for 10 days. Error bars denote ± SEM, n ≥ 18, and means labeled with different letters are significantly different at $p < 0.05$, Dunnett's C (variance not neat).

bioRxiv preprint doi: https://doi.org/10.1101/2023.01.24.525215; this version posted January 24, 2023. The copyright holder for this preprint (which was not certified by peer review) is the author/funder. All rights reserved. No reuse allowed without permission.

Docking simulations of evk and RBOHD/RBOHF

Our experimental results indicated that the evk-mediated ROS burst is dependent on RBOHD and RBOHF, but how evk interacts with RBOHD/RBOHF is still unknown. Therefore, docking simulation was carried out to explore their binding mode. The 3D structures of RBOHD/RBOHF were built with SwissModel firstly. And then the possible binding sites of RBOHD/RBOHF were explored with Site Finder in Molecular Operating Environment (MOE). The top two recommended binding sites were used as binding sites of RBOHD/RBOHF, which are corresponding to the FAD (site1) and/or NADPH binding site (site2) of the highly homologous human DUOX1-DUOXA1 (dual oxidase 1 and dual oxidase maturation factor 1)[63] and Cylindrospermum stagnale NADPH oxidase 5 (NOX5)[64]. In the NADPH oxidase, NADPH works as an electron donor and FAD as an electron transporter, which passes electron sequentially to the two heme molecules and then to oxygen molecule, and forms superoxide anion finally[65]. So evk was predicted inducing ROS production by assisting electron transfer, their possible binding modes were shown in figure 2.

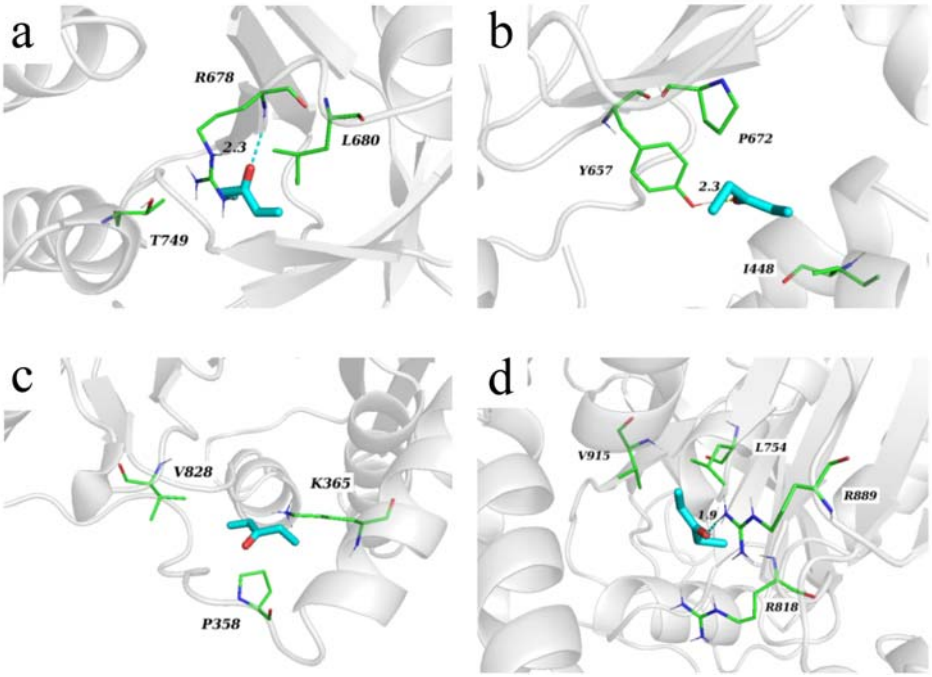

Figure 2. The structural docking model of evk (cyan sticks) binding on site1 (a) or site2 (c) of RBOHD, site1 (b) or site2 (d) of RBOHF (white cartoon) and, and the key residues labelled out in green sticks, and the hydrogen bond interactions labelled out in dash line.

As shown in Fig. 2a, evk bound to site1 of RBOHD by forming hydrogen bond interaction with Arg-678, hydrophorbic interactions with Leu-680, Thr-749. And evk bound to site1 of RBOHF (Fig. 2b) by forming hydrogen bond interaction with Tyr-657, hydrophorbic interactions with Pro-672, Ile-448. Besides, evk can bind with RBOHD on site2 (Fig. 2c) by forming hydrophorbic interaction with Pro-358, Lys-365, Val-828; or bound with RBOHF on site2 (Fig. 2d) by forming hydrogen bond interactions with Arg-889, forming hydrophorbic interactions with Leu-754, Val-915. Based on the docking simulation results, evk was predicted to assist electrons transfer of RBOHD/RBOHF by binding to their FAD or NADPH binding site, and thus inducing ROS production.

bioRxiv preprint doi: https://doi.org/10.1101/2023.01.24.525215; this version posted January 24, 2023. The copyright holder for this preprint (which was not certified by peer review) is the author/funder. All rights reserved. No reuse allowed without permission.

RBOH participates in the evk-induced increase in intracellular calcium concentrations

We used confocal laser scanning microscopy to detect intracellular Ca^{2+} levels based on Fluo3-AM fluorescence intensity. Compared to the control, the fluorescence intensity of Fluo3-AM increased by 183.9% (20 s), 189.2% (40 s), 132.1% (60 s), 124.3% (80 s), and 119.4% (100 s) into evk treatment. Ca^{2+} fluorescence was substantially lower in the WT pretreated with ruthenium red and *rbohd rbohf* cells plus evk than in WT cells exposed to evk (Figure 3a). We determined that the intracellular calcium pool is the source of the evk-induced calcium signal, as the fluorescence intensity of intracellular Ca^{2+} Fluo3-AM decreased by 118.6% in *rbohd rbohf* compared to the control after 40 s (Figure 3b). These results indicate that NADPHase affects the evk-induced calcium burst, whereas the evk-mediated H_2O_2 burst is unaffected by intracellular calcium pool inhibitors, indicating that H_2O_2 functions upstream of calcium signaling.

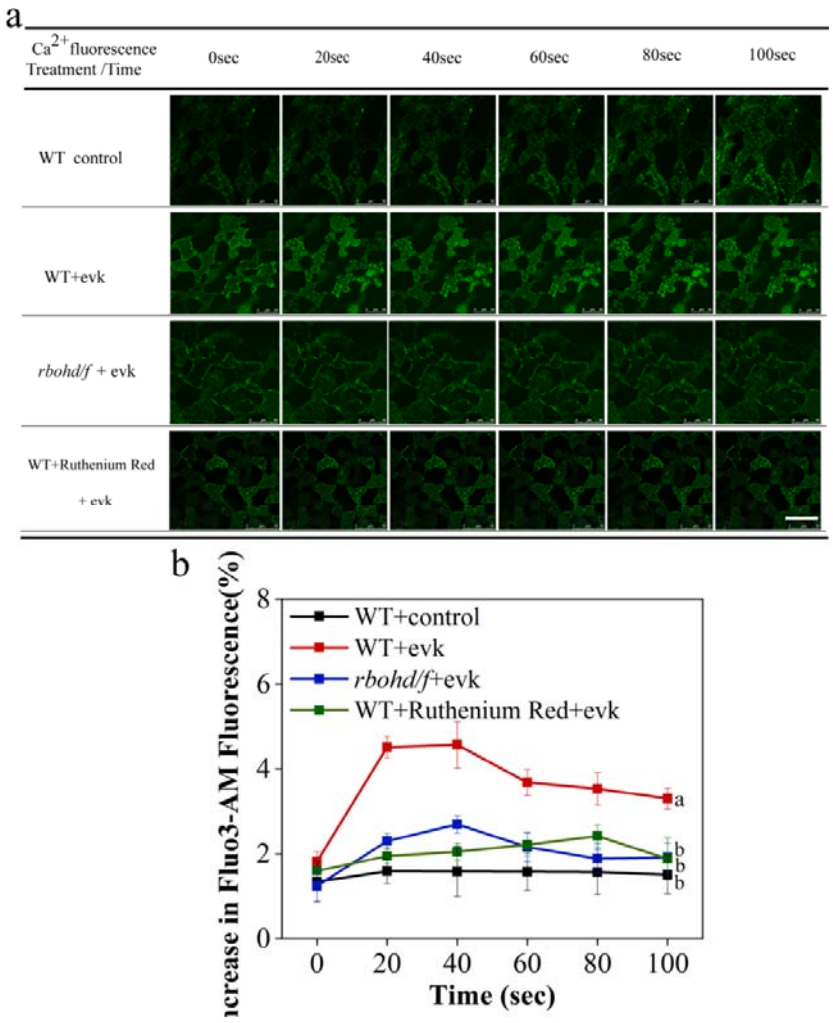

Figure 3. evk-induced increases in intracellular calcium levels depend on RBOHD RBOHF and internal Ca^{2+} release channels in Arabidopsis mesophyll cells. (a) The cells were washed to remove the 10 μM Fluo3-AM test solution (0 min), evk was added, and the cells were photographed every 30 s. Scale bars, 50 μm. (b) evk-induced increases in Ca^{2+} fluorescence are blocked in ruthenium red–treated WT and *rbohd rbohf* cells compared to WT + evk cells. The seedlings were grown for 10 days. Error bars denote ± SEM, n ≥ 19, and means labeled with different letters are significantly different at $p < 0.05$, Dunnett's C (variance not neat).

bioRxiv preprint doi: https://doi.org/10.1101/2023.01.24.525215; this version posted January 24, 2023. The copyright holder for this preprint (which was not certified by peer review) is the author/funder. All rights reserved. No reuse allowed without permission.

RBOH participates in evk-mediated calcium efflux

NMT revealed that treating Arabidopsis mesophyll cells with transient evk results in an intense efflux of transmembrane calcium ions from mesophyll cells. The efflux flow rate reached 261.11 ± 20.57 pmol cm^{-2} s^{-1} and then gradually returned to the resting state. To explore the role of NADPHase in Ca^{2+} efflux induced by evk, we examined the NADPHase mutant *rbohd rbohf* to detect changes in Ca^{2+} flow after evk treatment. Evk-induced Ca^{2+} efflux was weaker in *rbohd rbohf* compared to WT (Figure 4a). Immediately after the addition of evk, the calcium ion efflux flow rate was 111.83 ± 24.11 pmol cm^{-2} s^{-1}. The peak calcium efflux in WT and *rbohd rbohf* plants was 237.19 ± 15.31 pmol cm^{-2} s^{-1} and 58.95 ± 16.37 pmol cm^{-2} s^{-1}, respectively (Figure 4b), indicating that calcium efflux was significantly reduced in the mutant. These results indicate that RBOHD and RBOHF are involved in evk-induced calcium efflux in mesophyll cells.

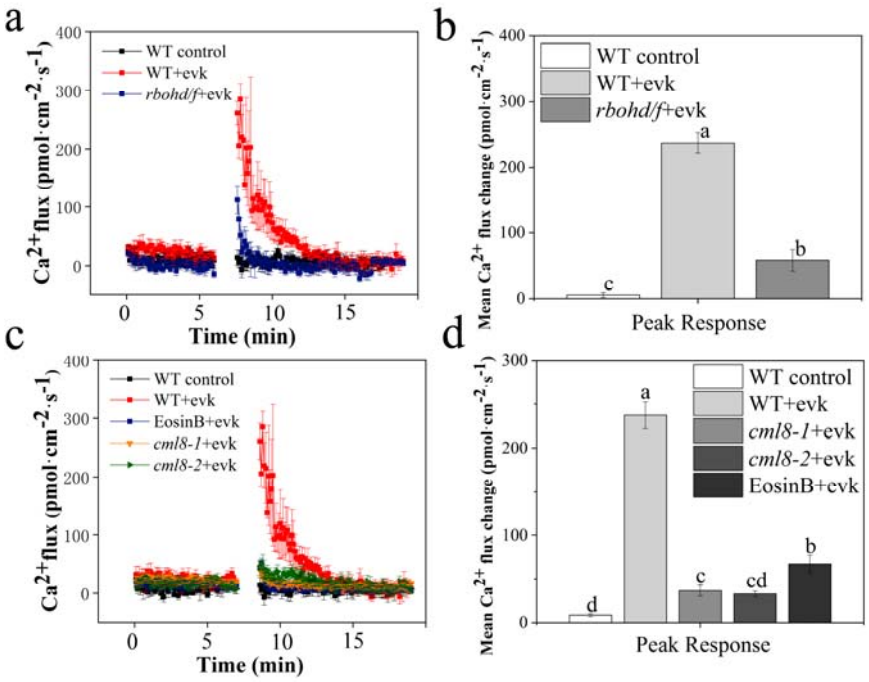

Figure 4. evk-induced Ca^{2+} efflux is enhanced by H_2O_2 and suppressed in eosin B–pretreated WT and *cml8* plants. (a,c) evk treatment increases Ca^{2+}efflux in WT, but not in *rbohd rbohf*, *cml8-1*, or *cml8-2*. (b,d) Peaks in mean Ca^{2+} efflux among genotypes and treatments, showing that Ca^{2+} efflux is significantly suppressed in all groups compared to the evk-treated WT control. The plants were grown for 3 weeks. Error bars denote ± SEM, n ≥ 6, and columns labeled with different letters are significantly different at $p < 0.05$, Dunnett's C (variance not neat).

CML8 interacts with ACA8 to regulate evk-induced calcium efflux

Eosin B is an inhibitor of calcium pumps. We therefore pretreated mesophyll cells with 10 μM eosin B, followed by evk treatment. Calcium ion efflux was significantly lower upon treatment with eosin B, reaching a peak value of 102.39 ± 23.73 pmol cm^{-2} s^{-1} and a peak calcium efflux value of 67.28 ± 10.34 pmol cm^{-2} s^{-1}, which was significantly lower than the peak value of the WT + evk group (237.19 ± 15.31 pmol cm^{-2} s^{-1}), indicating that the calcium pump plays a role in

bioRxiv preprint doi: https://doi.org/10.1101/2023.01.24.525215; this version posted January 24, 2023. The copyright holder for this preprint (which was not certified by peer review) is the author/funder. All rights reserved. No reuse allowed without permission.

evk-mediated calcium ion efflux from mesophyll cells. The *cml8-1* and *cml8-2* mutants also showed lower calcium ion efflux in mesophyll cells under evk treatment, with peak values of 44.27 ± 2.47 pmol cm^{-2} s^{-1} and 43.64 ± 12.48 pmol cm^{-2} s^{-1}, respectively (Figure 4c). The peak calcium efflux values in *cml8-1* and *cml8-2* were 36.48 ± 6.21 pmol cm^{-2} s^{-1} and 32.85 ± 3.20 pmol cm^{-2} s^{-1}, respectively, which were significantly lower than the peak value of the WT + evk group (Figure 4d). These results indicate that CML8 regulates calcium pump function during evk-mediated calcium ion efflux, thus affecting calcium efflux. We established that the calcium-dependent ATPase ACA8 is the likely target of CML8 regulation, as demonstrated by its interaction in yeast two-hybrid, firefly luciferase complementation imaging, and pull-down assays (Figure 5a-5c).

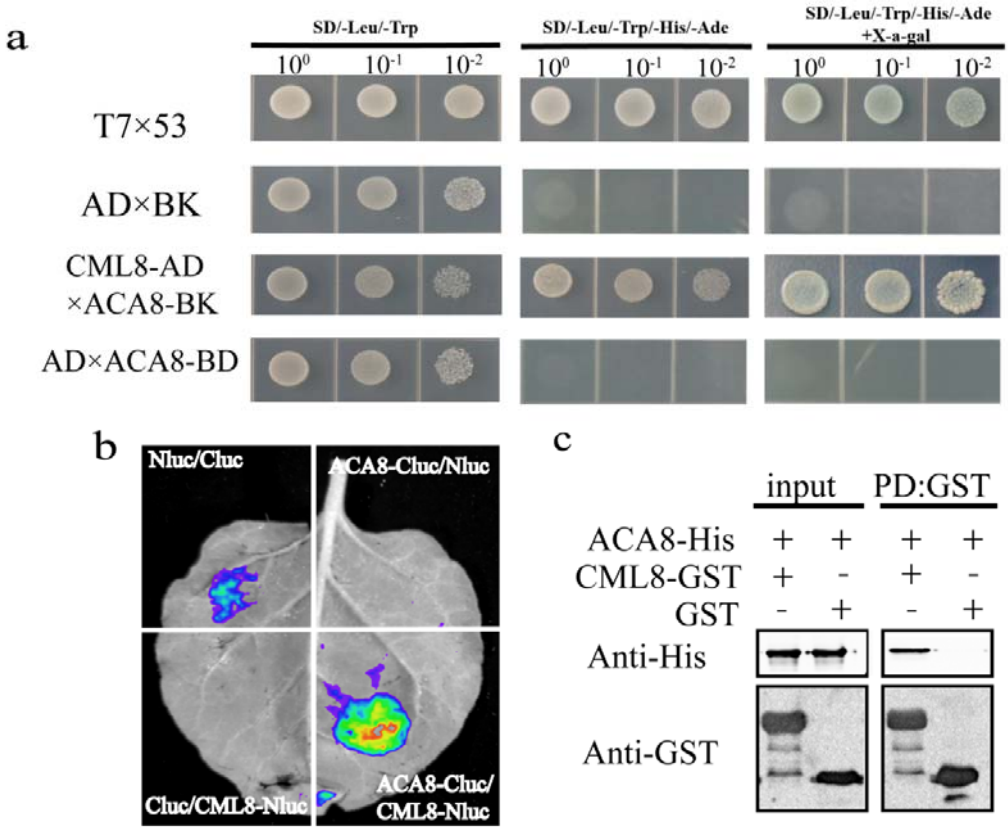

Figure 5. CML8 interacts with ACA8

(a) Yeast two-hybrid assay showing that ACA8 interacts with CML8. Yeast colonies harboring the indicated constructs were grown on synthetic defined (SD) medium lacking Trp and Leu, or SD medium lacking Trp, Leu, His, and Ade. (b) Firefly luciferase complementation imaging assay. *N. benthamiana* leaves were infiltrated with the construct pairs *ACA8-CLuc/CML8-NLuc*, *Cluc/NLuc*, *ACA8-CLuc/NLuc*, and *CLuc/CML8-NLuc*. (d) *In vitro* pull-down assays. The N terminus (residues 1–180), an intracellular domain, was used to interact with CML8. GST-CML8 pulled down His-tagged ACA8, indicating that CML8 interacts with ACA8.

bioRxiv preprint doi: https://doi.org/10.1101/2023.01.24.525215; this version posted January 24, 2023. The copyright holder for this preprint (which was not certified by peer review) is the author/funder. All rights reserved. No reuse allowed without permission.

Evk mediates SA/JA antagonism in Arabidopsis

Evk activates the H_2O_2 burst. H_2O_2 and SA are strongly correlated, and *WRKY53* expression is strongly activated by evk, as revealed by reverse transcription quantitative PCR (RT-qPCR). Therefore, we reasoned that evk might activate SA-related gene expression. We measured the expression of SA-related genes via RT-qPCR. We observed that evk treatment upregulates *NPR1*, *NPR4*, *ICS1* (*ISOCHORISMATE SYNTHASE 1*), *PAD4* (*PHYTOALEXIN DEFICIENT 4*), and *SARD1* (*SAR DEFICIENT 1*), especially during the early stage of treatment (0 to 3 h). However, *PR1* was not only upregulated at 3 h, but it was still upregulated at 8 h, indicating that a regulatory substance activated *PR1* expression during the early and late stages of treatment. Most SA-related genes were downregulated in the later stage of treatment, suggesting that JA might antagonize their expression at this stage. However, the JA-related genes *OPR1* (*12-OXOPHYTODIENOATE REDUCTASE 1*), *OPR3*, *AOC3* (*ALLENE OXIDE CYCLASE 3*), *JMT* (*JASMONIC ACID CARBOXYL METHYLTRANSFERASE*), *LOX2*, and *PDF1.2* were strongly upregulated during the later stage of evk treatment (3 to 8 h). RT-qPCR showed that evk treatment antagonizes SA/JA signaling, especially the simultaneous activation of *PR1* and *PDF1.2* expression at 8 h. The finding that *PR1* and *PDF1.2* are both upregulated at the later stage of treatment (Figure 6a,6b) is intriguing. In addition, the plants accumulated more SA within 3 h of evk treatment. During the later stage of treatment (8 h), the SA content remained high, and the JA level increased (Figure 6c).

CAM5 functions upstream of WRKY53 in evk signaling

RT-qPCR analysis showed that *WRKY53* expression begins to decline after 1 h of upregulation (Figure 6e). We examined *CAM5* expression during early evk treatment (90 min) because the calcium signal is an early signal. *CAM5* was upregulated at all time points during the early stage of evk treatment (Figure 6d). We also measured *WRKY53* expression in the *cam5* mutant. *WRKY53* expression was much lower in the mutant. On the contrary, *CAM5* expression was not affected in the *wrky53* mutant (Figure 6d,6e). These results indicate that CAM5 functions upstream of WRKY53 in response to evk treatment.

bioRxiv preprint doi: https://doi.org/10.1101/2023.01.24.525215; this version posted January 24, 2023. The copyright holder for this preprint (which was not certified by peer review) is the author/funder. All rights reserved. No reuse allowed without permission.

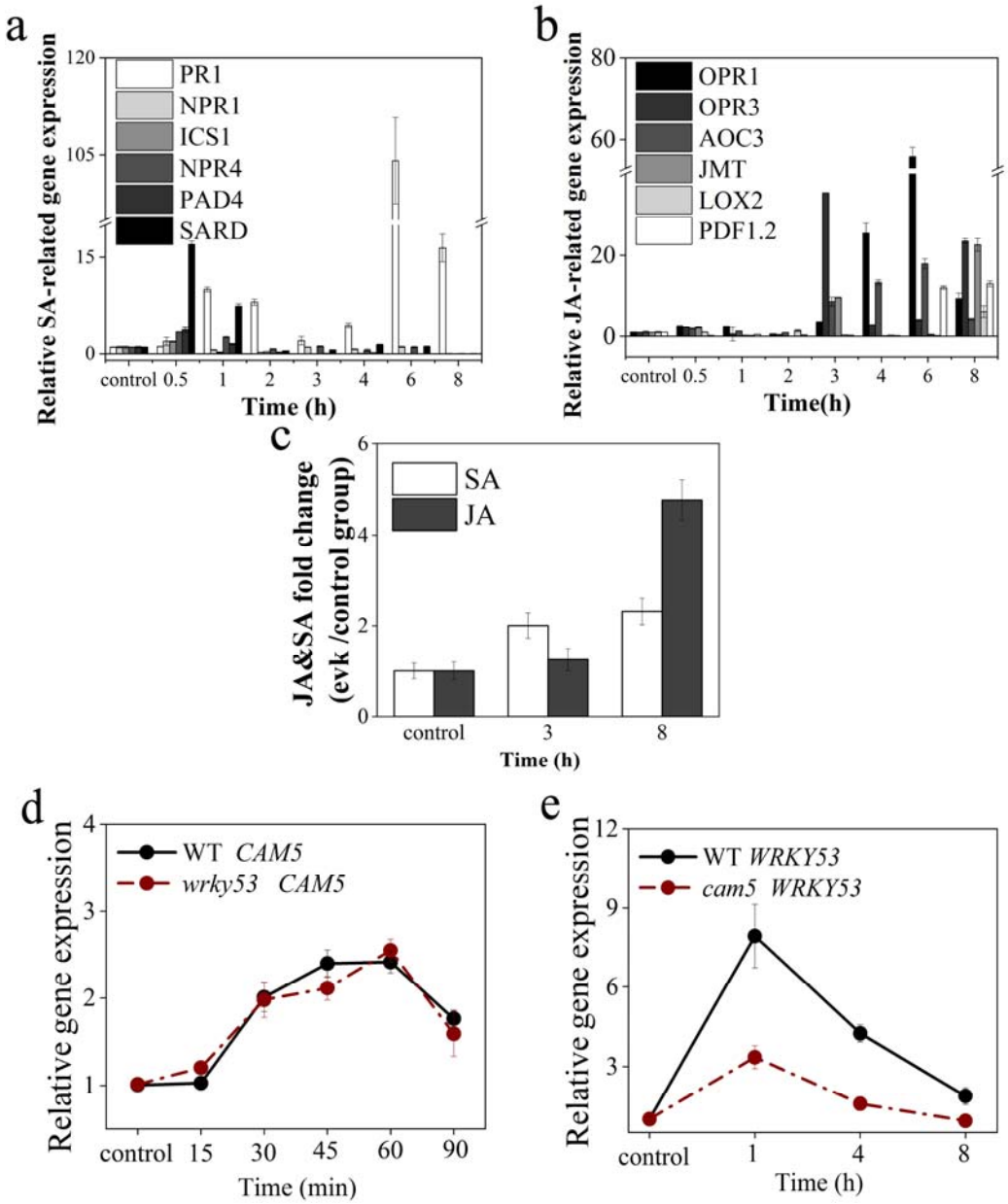

Figure 6. Evk-induced changes in gene expression.

(a,b) Expression levels of key SA/JA-related genes in WT plants following evk treatment. The plants were grown for 3 weeks. Data are means ± SEM, n ≥ 3. (c) evk-induced fold-change in JA and SA levels. (d) Relative *CAM5* expression levels in the leaves of 2-week-old WT and *wrky53* seedlings. (e) Relative *WRKY53* expression levels in the leaves of 2-week-old WT and *cam5* seedlings. The seedlings were grown for 3 weeks. Data are means ± SEM, n ≥ 3.

CAM5 and WRKY53 positively regulate the expression of SA-related genes and negatively regulate the expression of JA-related genes

Within 3 h of evk treatment, *PR1*, *NPR4*, and *SARD* were significantly upregulated in the WT but significantly downregulated in *wrky53* and *cam5* (Figure 7e,7f,7g), indicating that WRKY53 and CAM5 positively regulate the evk-induced activation of *PR1*, *NPR4*, and *SARD1*. After 3 h of evk

bioRxiv preprint doi: https://doi.org/10.1101/2023.01.24.525215; this version posted January 24, 2023. The copyright holder for this preprint (which was not certified by peer review) is the author/funder. All rights reserved. No reuse allowed without permission.

treatment, JA-related genes were significantly upregulated, especially *OPR1*, *OPR3*, *JMT*, and *AOC3* (Figure 7a,7b,7c,7d). Notably, in *wrky53*, the upregulation of these genes was more obvious, indicating that WRKY53 negatively regulates JA-related gene expression. When *WRKY53* was mutated, we detected little evk-induced upregulation of *PR1*. On the contrary, *PDF1.2* was significantly upregulated during the late stage of evk treatment, indicating that WRKY53 is likely a positive regulator of *PR1* and a negative regulator of *PDF1.2* (Figure 7h,7i).

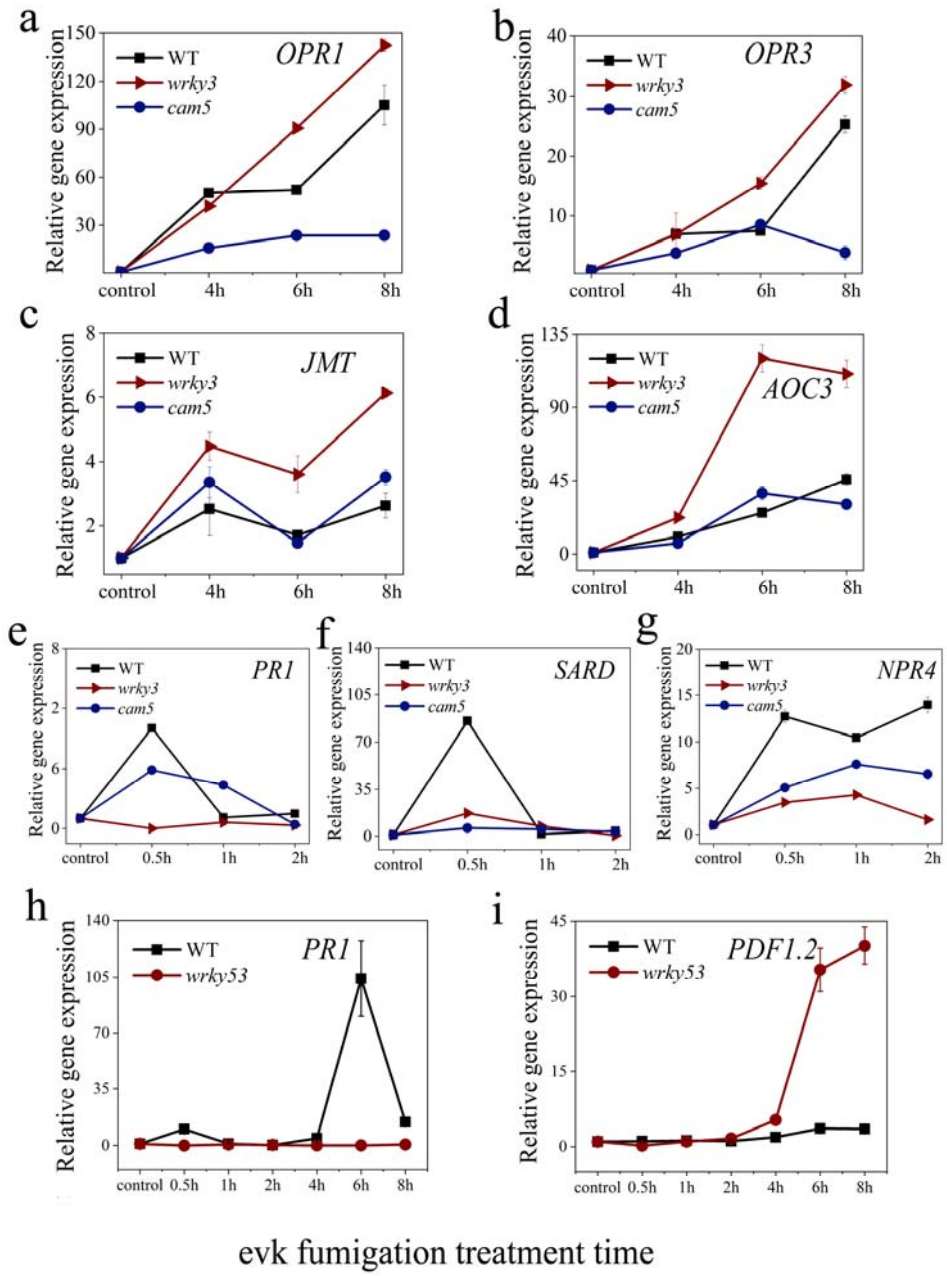

Figure 7. Evk-induced changes in SA/JA-related gene expression in WT, *wrky53*, and *cam5* plants

(a-d) Relative expression levels of JA-related genes in the leaves of WT, *wrky53*, and *cam5* plants following evk treatment. (e-g) Relative expression levels of SA-related genes in the leaves of WT, *wrky53*, and *cam5* plants following evk treatment. (h,i) Relative expression levels of *PR1* and *PDF1.2* in the leaves of WT and *wrky53* plants following evk treatment. The plants were grown for 3 weeks. Data are means ± SEM, n ≥ 3.

bioRxiv preprint doi: https://doi.org/10.1101/2023.01.24.525215; this version posted January 24, 2023. The copyright holder for this preprint (which was not certified by peer review) is the author/funder. All rights reserved. No reuse allowed without permission.

CAM5 interacts with WRKY53, and increasing calcium concentrations weaken this interaction

Evk treatment upregulated the expression of SA-related genes, which was strongly associated with both WRKY53 and CAM5, and CAM5 regulates the expression of *WRKY53*, suggesting that WRKY53 and CAM5 might interact. In yeast two-hybrid assays, yeast cells harboring CAM5-AD and WRKY53-BD (amino acids [aa] 1–217) grew well on selective medium, and the colonies turned blue on X-gal plates, indicating that these two proteins indeed physically interact (Figure 8a). In a luciferase complementation test (Figure 8c), *Nicotiana benthamiana* leaves transiently expressing *CAM5-NLuc* + *WRKY53-CLuc* constructs had stronger luminescence than the *NLuc* + *CLuc*, *CAM5-NLuc* + *CLuc*, or *WRKY53-CLuc* + *NLuc* combinations (Figure 8c), confirming that CAM5 and WRKY53 interact. Finally, in a glutathione S-transferase (GST) pull-down experiment, recombinant CAM5-GST pulled down WRKY53-His (Figure 7d). In response to increasing calcium ion concentrations, the amount of WRKY53 pulled down by CAM5-GST gradually decreased. In the presence of EGTA, CAM5-GST pulled down the greatest amount of WRKY53 (Figure 8b). These results indicate that WRKY53 is released from the CAM5-WRKY53 complex in the presence of increasing calcium concentrations.

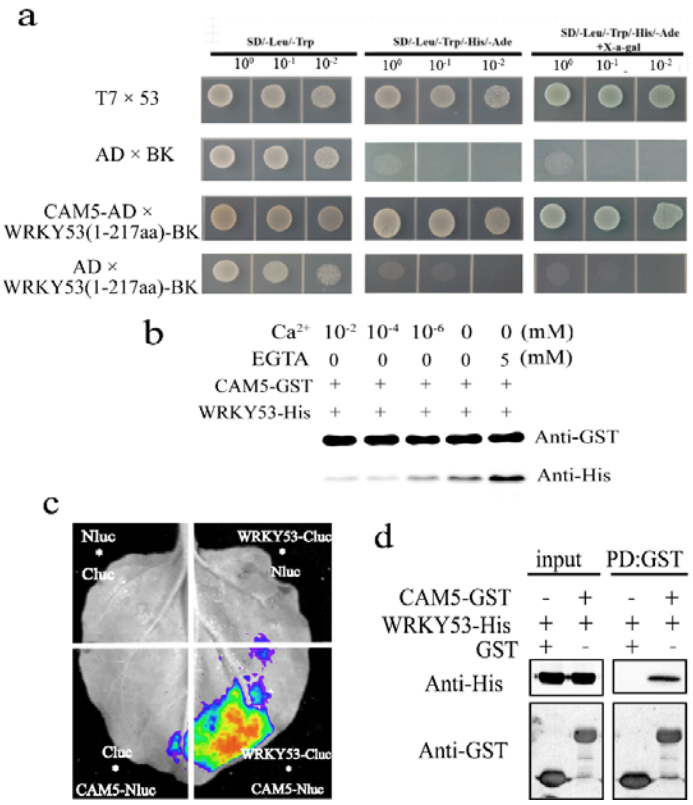

Figure 8. CAM5 interacts with WRKY53

(a) Yeast two-hybrid assay; the N terminus of WRKY53 (residues 1–217) was used as bait. Yeast cells harboring CAM5-AD and WRKY53-BD (aa 1–217) grew normally on all plates. (b) Pull-down assay showing the effects of calcium concentration on the binding of WRKY53 to CAM5. (c) LCI assay showing the interaction between WRKY53 and CAM5. *N. benthamiana* leaves were infiltrated with the pairs of constructs *WRKY53-CLuc/CAM5-NLuc*, *CLuc/NLuc*, *WRKY53-CLuc/NLuc*, or *CLuc/CAM5-NLuc*. (d) GST pull-down assay showing that GST-CAM5 binds to WRKY53- His.

bioRxiv preprint doi: https://doi.org/10.1101/2023.01.24.525215; this version posted January 24, 2023. The copyright holder for this preprint (which was not certified by peer review) is the author/funder. All rights reserved. No reuse allowed without permission.

549

550 **TGA5 interacts with WRKY53**

551 We hypothesized that TGA5, a transcription factor that responds to RES, might be involved in the
552 late stage of the response to evk treatment by upregulating *PR1* after the downregulation of
553 *WRKY53*. In a luciferase complementation test, we detected higher luciferase activity from *N.*
554 *benthamiana* leaves co-infiltrated with the constructs *TGA5-CLuc* + *WRKY53-NLuc* than with the
555 pairs *NLuc* + *CLuc*, *TGA5-CLuc* + *NLuc*, and *WRKY53-NLuc* + *CLuc* (Figure 9b), indicating that
556 TGA5 and WRKY53 interact. In a GST pull-down assay, recombinant TGA5-GST pulled down
557 WRKY53-His (Figure 9a). We also established that TGA5 interacts with WRKY53 in the nucleus,
558 as demonstrated by BiFC (Figure 9c). These results demonstrate that TGA5 and WRKY53 interact
559 *in vitro* and *in vivo*.

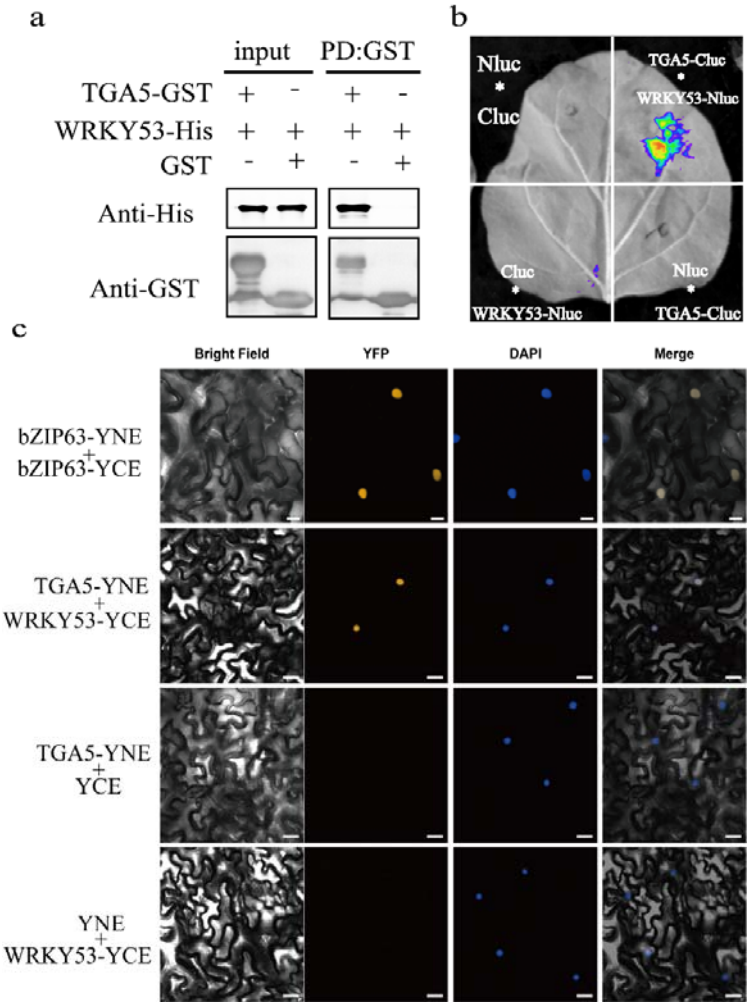

560

561 **Figure 9.** WRKY53 interacts with TGA5

562 (a) TGA5-GST pulls down WRKY53-His *in vitro*. (b) LCI assay showing that WRKY53 and CAM5 interact *in*
563 *vivo*. *N. benthamiana* leaves were infiltrated with the pairs of constructs *WRKY53-CLuc/CAM5-NLuc*, *CLuc/NLuc*,
564 *WRKY53-CLuc/NLuc*, and *CLuc/CAM5-NLuc*. (c) BiFC assays indicating that TGA5 interacts with WRKY53 in
565 the nucleus.

566

567

bioRxiv preprint doi: https://doi.org/10.1101/2023.01.24.525215; this version posted January 24, 2023. The copyright holder for this preprint (which was not certified by peer review) is the author/funder. All rights reserved. No reuse allowed without permission.

WRKY53 enhances the binding of TGA5 to *PR1* and weakens its binding to *PDF1.2*

We performed EMSAs to test whether WRKY53 might bind to the *PR1* promoter. Accordingly, we labeled a promoter fragment of *PR1* with biotin and incubated the resulting probe with recombinant purified His-WRKY53. We observed that WRKY53 directly binds to the w-box in the *PR1* promoter, whereas CAM5 did not (Figure 10a). In the presence of both WRKY53 and CAM5, the binding of WRKY53 to the w-box of the *PR1* promoter was weakened. When calcium ions were added to the system, the binding of WRKY53 to the w-box was restored (Figure 10a). To determine whether TGA5 also bound to the w-box in the *PR1* promoter, we performed another EMSA with recombinant TGA5-MBP (maltose-binding protein), finding that TGA5 directly binds to the w-box in the *PR1* promoter. In the presence of both WRKY53 and TGA5, WRKY53 appeared to enhance the binding strength of TGA5 to this w-box. These results indicate that WRKY53 promotes the binding of TGA5 to the w-box in the *PR1* promoter (Figure 10b). Moreover, WRKY53 bound to the w-box in the *PDF1.2* promoter, whereas CAM5 did not (Figure 10c). In the presence of both WRKY53 and CAM5, the binding of WRKY53 to the w-box in the *PDF1.2* promoter was weakened. When calcium ions were added to this system, the original binding strength of WRKY53 to the w-box in the *PDF1.2* promoter was restored (Figure 10c). WRKY53 failed to bind to the as-1 sequence in the *PDF1.2* promoter, but TGA5 bound to this sequence. In the presence of both WRKY53 and TGA5, WRKY53 weakened the binding of TGA5 to the as-1 sequence (Figure 10d).

In summary, when the calcium ion concentration increases, WRKY53 is released from the CAM5-WRKY53 complex, allowing it to interact with the downstream protein TGA5 to jointly regulate the expression of *PR1* and *PDF1.2*. WRKY53 enhances the binding strength of TGA5 to the w-box in the *PR1* promoter, while WRKY53 weakens the binding strength of TGA5 to as-1 in the *PDF1.2* promoter.

bioRxiv preprint doi: https://doi.org/10.1101/2023.01.24.525215; this version posted January 24, 2023. The copyright holder for this preprint (which was not certified by peer review) is the author/funder. All rights reserved. No reuse allowed without permission.

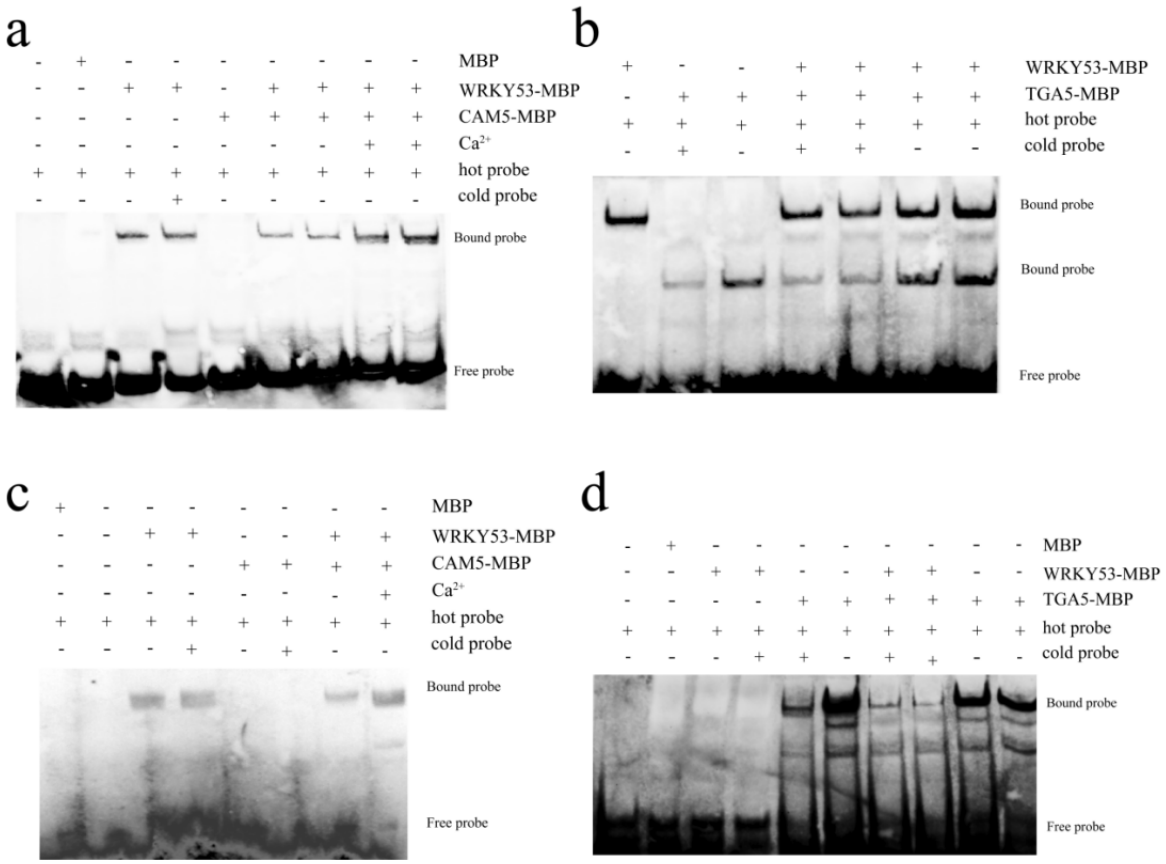

Figure 10. WRKY53 enhances the binding strength of TGA5 to the w-box in the *PR1* promoter, while WRKY53 weakens the binding strength of TGA5 to as-1 in the *PDF1.2* promoter

(a) Ca^{2+} and CAM5 influence the binding ability of recombinant WRKY53 to the *PR1* promoter, as determined by EMSA. Hot probe refers to biotin-labeled probe and cold probe to unlabeled probe. The Ca^{2+} concentration is 10 mM. (b) WRKY53 enhances the binding of TGA5 to the w-box in the *PR1* promoter. WRKY53 binds to the w-box sequence ((C/T)TGAC(T/C)) in the *PR1* promoter. TGA5 binds to the w-box in the *PR1* promoter. WRKY53 enhances the binding of TGA5 to the w-box in the *PR1* promoter. The w-box sequence (C/T)TGAC(T/C) overlaps with the action center element as-1 (TGAC) of TGA. (c) Ca^{2+} and CAM5 influence the binding of WRKY53 to the *PDF1.2* promoter. (d) WRKY53 weakens the binding of TGA5 to the as-1 sequence in the *PDF1.2* promoter.

Dual-luciferase reporter assay

Finally, to verify that WRKY53 and TGA5 activate the promoters of their downstream genes, we performed transient expression assays in Arabidopsis protoplasts and *N. benthamiana* leaves. To this end, we cloned the *PR1* promoter into pGreenII0800-LUC to generate the luciferase (LUC) reporter construct. In parallel, we cloned the coding sequences of *WRKY53* and *TGA5* in the pGreenII 62-SK vector to generate the effector constructs, using *35S:REN* as an internal control for transfection or infiltration efficiency. The luciferase activation assay showed that WRKY53 and TGA5 induce *PR1* transcription, while only TGA5 induced *PDF1.2* transcription, and only WRKY53 repressed *PDF1.2* transcription. We then examined the activity of the effectors

bioRxiv preprint doi: https://doi.org/10.1101/2023.01.24.525215; this version posted January 24, 2023. The copyright holder for this preprint (which was not certified by peer review) is the author/funder. All rights reserved. No reuse allowed without permission.

WRKY53 and *TGA5* in regulating the *PR1* and *PDF1.2* promoters when co-expressed. We observed that WRKY53 cooperates with TGA5 to positively regulate *PR1* transcription (Figure 11c, 11d). Similarly, we determined that TGA5 inhibits the induction of *PDF1.2* transcription mediated by WRKY53 (Figure 11e, 11f).

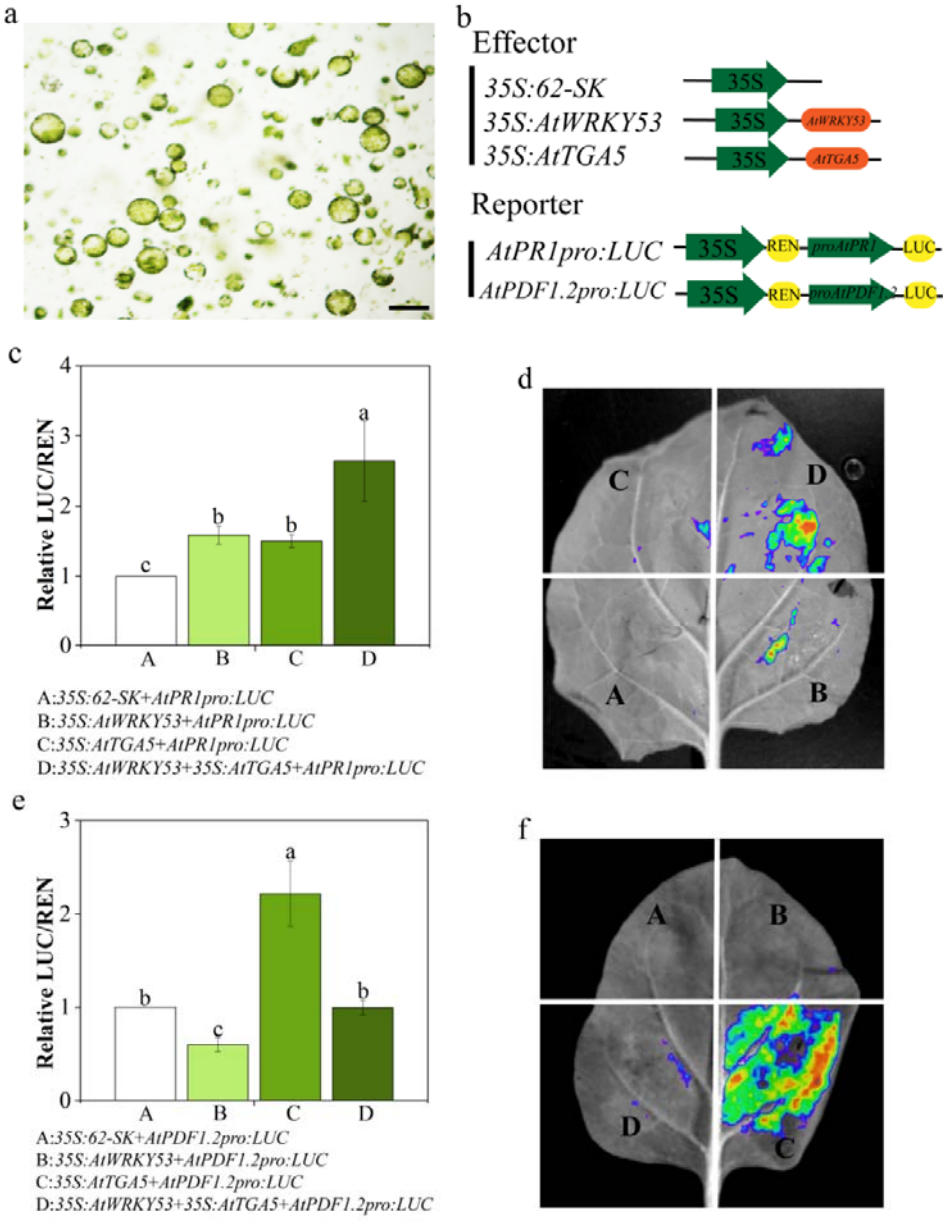

Figure 11. Luciferase activation assay. (a) Protoplasts extracted from 5-week-old Arabidopsis leaves. (b) Schematic diagrams of the effector and reporter constructs used for the dual-luciferase assay. (c,e) Dual-luciferase assay. Arabidopsis protoplasts were transiently transfected with the indicated constructs. Relative luciferase activity is shown as the ratio of LUC to REN activity. *35S:REN* (in pGreenII 62-SK) was used as an internal control. Error bars denote ± SEM, n ≥ 16, and means labeled with different letters are significantly different at $p < 0.05$, Dunnett's C (variance not neat). (d,f) Transient infiltration assay of *N. benthamiana* leaves with the indicated constructs.

bioRxiv preprint doi: https://doi.org/10.1101/2023.01.24.525215; this version posted January 24, 2023. The copyright holder for this preprint (which was not certified by peer review) is the author/funder. All rights reserved. No reuse allowed without permission.

Discussion

When a herbivore damages the leaves of a plant, volatile compounds such as terpenoids, C6-volatiles, and electrophiles are released. These compounds elicit a range of defense mechanisms in both the damaged plant and nearby plants. Infestation with lima bean mite (*Tetranychus urticae*) causes the release of terpenoid compounds, which in turn elicits the expression of defense genes in nearby plants (Arimura et al., 2000)[66]. These volatiles serve many purposes, including inducing pathogen-related (PR) protein activity and attracting natural herbivore predators[67]. Treatment with (Z)-3-hexenol also increases *PR* gene expression, indicating that (Z)-3-hexenol directly promotes a series of defense responses. evk is released as a pest-induced plant volatile when *Pieris rapae* is fed on Arabidopsis[68]. Evk is a small, volatile chemical molecule with an α, β-unsaturated carbonyl structure. Due to its unique functional group, this molecule is dispersed rapidly and has a strong ability for long-distance diffusion, making it an effective signaling molecule. In the current study, for the first time, we found the key proteins that sense evk through molecular docking. The recognition of volatiles and receptors is the starting point of defense signals, which is the key to the transmission of defense signals between plants and the cause of population resistance. Based on the docking simulation results, it is predicted that evk will assist the electron transfer of RBOHD/RBOHF by binding to its FAD or NADPH binding sites (Figure 2). When the signal is recognized, we observed and characterized the whole process of evk mediated defense response: a. ROS burst; b. intracellular Ca^{2+} concentration change; c. WRKY53-CAM5 complex decomposing and release WRKY53; d. WRKY53 and TGA5 regulate expression of defense genes by evk.

Cytoplasmic free Ca^{2+} concentrations and H_2O_2 are thought to play crucial roles in the volatile-sensing mechanisms of plants, although these roles have not been directly demonstrated. We previously showed that evk is recognized by plants and induces H_2O_2 production, which ultimately mediates stomatal closure to reduce pathogen infection[69]. In the current study, we demonstrated that evk, a volatile compound released by plants, increased the levels of H_2O_2 and intracellular calcium in Arabidopsis mesophyll cells. CML8-ACA8 lowered the levels of intracellular calcium after the calcium ions have served their function, causing calcium levels in the cells to return to the resting state. H_2O_2 levels in mesophyll cells rose when Arabidopsis detected evk, with the H_2O_2 burst in leaves being mediated by NADPH oxidases. Therefore, H_2O_2 levels in mesophyll cells increased in an RBOHD- and RBOHF-dependent manner. Importantly, the evk-mediated ROS burst was unaffected by pretreatment with ruthenium red, which blocked membrane calcium fluxes (Figure 1a,1b).

Ca^{2+} homeostasis is tightly regulated in plant cells. The most abundant Ca^{2+} store in plant cells is the vacuole, with Ca^{2+} concentrations ranging from 0.2 to 5 mM[70]. Conversely, the chloroplast stroma contain <150 nM of free Ca^{2+}, similar to that in the cytosol[71]. Evk treatment rapidly increased intracellular Ca^{2+} concentrations (Figure 3a,3b) and Ca^{2+} flow, but both effects were reduced in *rbohd rbohf* mesophyll cells (Figure 4a,4b). These results suggested that the H_2O_2 burst induced by evk took place prior to the rise in Ca^{2+} levels in Arabidopsis mesophyll cells. Additionally, the increase in intracellular calcium levels was less severe in the ruthenium red pretreatment group, indicating that the intracellular calcium pool plays a role in the increase in intracellular calcium concentrations mediated by evk. Similar observations were made following treatment with evk and acyclic compounds[72,73]. By contrast, (E)-2-hexenal, an electrophilic compound, mainly promotes Ca^{2+}-influx from the extracellular space. Interestingly, ROS

bioRxiv preprint doi: https://doi.org/10.1101/2023.01.24.525215; this version posted January 24, 2023. The copyright holder for this preprint (which was not certified by peer review) is the author/funder. All rights reserved. No reuse allowed without permission.

669 scavengers attenuated the (E)-2-hexenal-induced intracellular calcium transient, suggesting that
670 ROS-dependent activation of plasma membrane Ca^{2+}-permeable channels participates in the
671 electrophile-dependent intracellular calcium transient[73].
672 Ca^{2+} and H_2O_2 collaborate during two processes in plants: Ca^{2+}-induced ROS generation and
673 Ca^{2+}-induced ROS release[29]. Here, we demonstrated how evk functioned as a signal transducer
674 during ROS-induced Ca^{2+} release. Different stimuli are detected by various mechanisms
675 throughout early signal transmission, making the sequence of early signal transmission events a
676 unique "language" in plant resistance. Ca^{2+} is crucial for many signaling cascades, yet excessive
677 amounts of Ca^{2+} in the cytoplasm are harmful to living organisms. The intracellular Ca^{2+} storage
678 membrane and the plasma membrane both carry Type P ATPases, which take part in Ca^{2+} efflux.
679 CaM can only be coupled with II B Ca^{2+}-ATPases. CaM attaches to the N-terminal CaM-binding
680 site when the N terminus of Ca^{2+} ATPases binds to Ca^{2+}[74]. We discovered that mesophyll cells
681 treated with evk had potent Ca^{2+} outflow by measuring the Ca^{2+} flux. We therefore investigated the
682 possibility that the Ca^{2+} ATPase inhibitor eosin B would prevent this Ca^{2+}efflux. Our findings
683 demonstrated that Ca^{2+} ATPase contributed to the Ca^{2+}efflux of mesophyll cells induced by evk
684 and that Ca^{2+} efflux was blocked in *cml8* plants (Fig. 3c,3d). We hypothesize that the restoration of
685 Ca^{2+} levels during the resting stage is mediated by an interaction between CML8 and ACA8 (Fig.
686 5a-5c).
687 Plants have developed sophisticated defense mechanisms against necrotrophic and biotrophic
688 diseases[75]. Plants typically activate JA-induced defense responses against herbivorous insects or
689 necrotrophic pathogens. Infection by *Pseudomonas syringae* pv. *tomato* DC3000 induces plants to
690 accumulate SA, which promotes the interaction of NPR1 with TGA transcription factors and
691 modulates the expression of pathogenesis-related (*PR*) genes. Plants activate SA-mediated
692 resistance against biotrophic pathogens. *B. cinerea* infection activates JA biosynthesis and
693 signaling pathways to promote the immune response[76]. These JA-related transcription factors then
694 activate JA-responsive genes such as *PDF1.2* against necrotrophs[46].
695 The cell redox status shifts due to the presence of the unsaturated carbonyl group of evk,
696 which is highly oxidizable. The major plant hormone SA is extremely redox state sensitive, and
697 evk triggers an H_2O_2 burst. Since there is a significant correlation between H_2O_2 and SA and
698 WRKY53 is substantially activated by evk, as determined by RT-qPCR (Figure. 6d), we reasoned
699 that evk might activate genes related to SA. We therefore performed RT-qPCR to examine the
700 expression of all SA-related genes. evk treatment (particularly during the first 3 h) greatly
701 stimulated the expression of SA-related genes (Figure 6a). This treatment also blocked the
702 expression of several JA-related genes (Figure 6b). JA levels rapidly increased within 8 h of
703 treatment, and SA accumulation increased dramatically at 3 h and remained unchanged at 8 h
704 (Figure. 6c).
705 Interestingly, however, *PR1* was upregulated not only at 3 h but also at 8 h of evk treatment,
706 suggesting that a regulator activates *PR* expression during both the early and late stages of
707 treatment. As demonstrated by RT-qPCR, evk treatment of Arabidopsis leaves induced SA/JA
708 antagonism, particularly the simultaneous activation of the defense genes *PR1* and *PDF1.2* at 8 h
709 (Figure 6a,6b). evk treatment increased SA/JA levels in addition to triggering the antagonism of
710 SA/JA. *PR1* and *PDF1.2* were previously found to be antagonistically activated; however, under
711 evk treatment, they may become co-activated at a later time.
712 JA and SA act antagonistically to mediate defense responses: JA can repress SA-mediated

bioRxiv preprint doi: https://doi.org/10.1101/2023.01.24.525215; this version posted January 24, 2023. The copyright holder for this preprint (which was not certified by peer review) is the author/funder. All rights reserved. No reuse allowed without permission.

713 defense[77]. SA also affects the expression of the genes encoding the JA biosynthesis enzymes
714 LOX2 and AOS[78,79]. Several components of SA signaling also suppress JA signaling, including
715 NPR1, the glutaredoxin GRX480, and class II TGA and WRKY transcription factors[79,80]. SA
716 strongly reduces the accumulation of ORA59 (OCTADECANOID-RESPONSIVE
717 ARABIDOPSIS AP2/ERF 59), a JA-responsive transcription factor, thereby inhibiting the
718 expression of JA-responsive genes[80]. Biotrophic pathogen-induced SA accumulation inhibits
719 CAT2 activity to inhibit JA accumulation by ACX2 and ACX3[81].
720 In the current study, whereas SA-related gene expression was substantially elevated during
721 the early stages of evk treatment, this expression was suppressed during the later stages, while
722 JA-related genes were strongly induced. Whereas JA levels only increased during the late stage of
723 evk treatment, SA was maintained at high levels, which were relatively constant in both the early
724 and late stages. In particular, when *WRKY53* was mutated, we detected almost no *PR1* expression,
725 whereas *PDF1.2* was significantly upregulated during the later stage of evk treatment (Figure.
726 7h,7i). Therefore, it is highly likely that WRKY53 serves as a node of SA/JA antagonism.
727 When *CAM5* or *WRKY53* was mutated, SA-related genes were downregulated (Figure.
728 7e-7g), indicating that CAM5-WRKY53 positively regulate the expression of these genes. In
729 addition, CAM5 positively regulated *WRKY53*. These findings confirm the notion that CAM5 and
730 WRKY53 interact and that the increase in calcium concentration causes WRKY53 to be released
731 from the CAM5-WRKY53 complex (Figure. 8a-8d).
732 *PR1* was not significantly upregulated in *wrky53*, but *PDF1.2* was highly upregulated in this
733 mutant. These findings indicate that WRKY53 is a key factor that positively regulates *PR1*
734 expression and negatively regulates *PDF1.2* expression (Figure. 7h,7i). The dual-luciferase
735 reporter assay further revealed that WRKY53 positively regulates *PR1* and negatively regulates
736 *PDF1.2* transcription (Figure. 11c-11f). In an RT-qPCR assay, after evk treatment, the expression
737 pattern of *WRKY53* showed a single peak, indicating that this gene was downregulated during the
738 later stage of treatment, suggesting that other factors are involved in *PR* activation. TGA5
739 positively activated *PR1* expression. The WRKY53-CAM5 complex was unlocked when
740 intracellular calcium levels rose following evk treatment (Figure. 8b). The freed WRKY53 was
741 then able to bind to the *PR1* and *PDF1.2* promoters, increasing and inhibiting their transcriptional
742 output, respectively (Figure 10a,10c; Figure 11c-11f). Additionally, the released WKY53 may
743 influence the capacity of TGA5 to bind to *PR1* and *PDF1.2*. The capacity of TGA5 to bind to the
744 as-1 motif in the *PR* promoter was enhanced by WRKY53 (Figure. 10b), whereas the ability of
745 TGA5 to bind to this element in the *PDF1.2* promoter was inhibited by WRKY53 (Figure. 10d).
746 As a result, WRKY53 greatly induced *PR1* expression while suppressing *PDF1.2* transcription.
747 This study established for the first time that WRKY53 positively activates *PR1* transcription while
748 negatively activating that of *PDF1.2*. However, WRKY53 reduced the binding capacity of TGA5
749 to the as-1 sequence and prevented the transcription of *PDF1.2* in the presence of both WRKY53
750 and TGA5. We discovered that *WRKY53* was expressed in a unimodal pattern, which explains why
751 *PDF1.2* expression was suppressed during the early stages of evk treatment and was triggered
752 when *WRKY53* expression decreased. *PR1* was undoubtedly activated during the early stages of
753 evk treatment, and why it was still upregulated during the later stages of treatment, when *WRKY53*
754 expression was lower, TGA5 still allows positive regulation of PR1 expression. Our findings
755 support the hypothesis that a novel factor, TGA5, is involved in *PR1* activation and that TGA5
756 continues to positively regulate *PR1* expression during the later stage of treatment with evk.

bioRxiv preprint doi: https://doi.org/10.1101/2023.01.24.525215; this version posted January 24, 2023. The copyright holder for this preprint (which was not certified by peer review) is the author/funder. All rights reserved. No reuse allowed without permission.

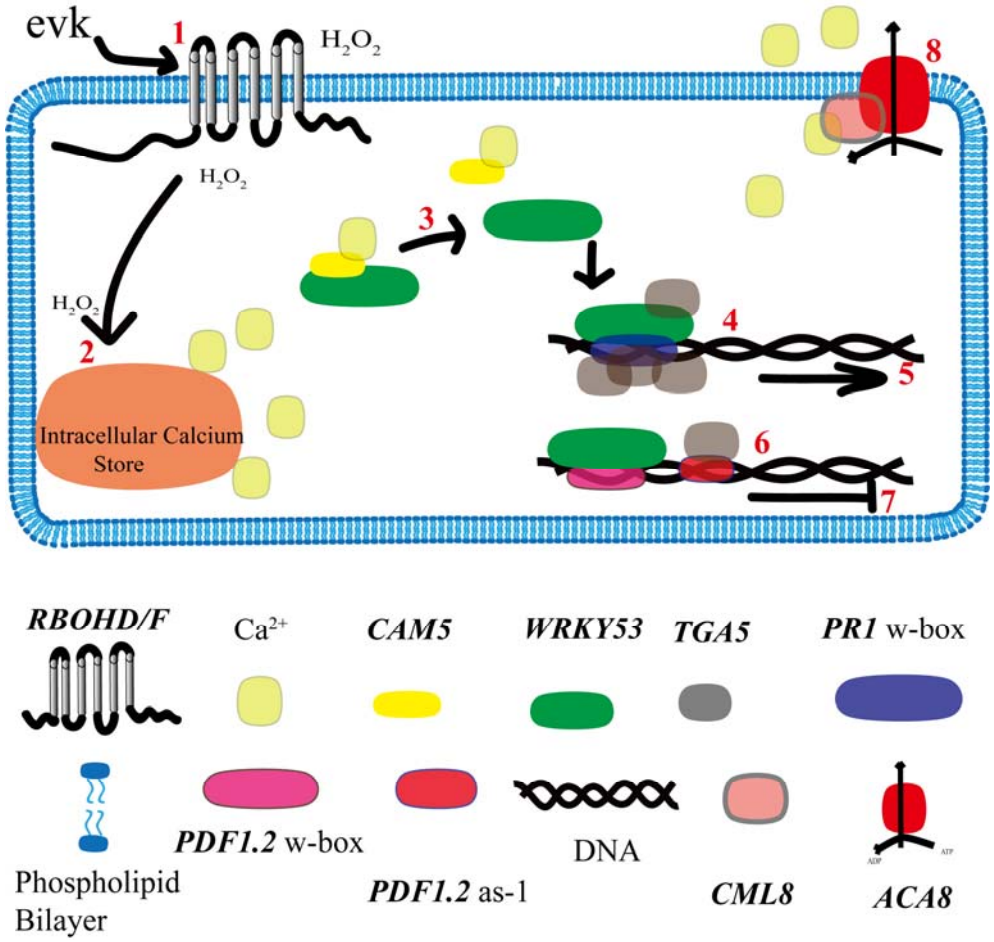

Figure 12. Schematic diagram of plant responses to evk.

(1) evk is recognized by plants and causes ROS release. (2) H_2O_2 mediates the release of calcium ions from the intracellular calcium pool and increases the intracellular calcium concentration. (3) The WRKY53-CAM5 complex is disrupted under high calcium concentrations. (4) WRKY53 binds to the w-box in the *PR1* promoter to induce its expression, and (5) WRKY53 enhances the binding of TGA5 to as-1 in the *PR1* promoter to enhance its expression. (6) WRKY53 binds to the w-box in the *PDF1.2* promoter to inhibit its expression, and (7) WRKY53 weakens the binding of TGA5 to as-1 in the *PDF7* promoter, thereby inhibiting its expression. When *WRKY53* expression decreases during the later period of evk treatment (8 h), the inhibition of *PDF1.2* is alleviated, thus significantly increasing *PDF1.2* expression. (8) Calcium ions are expelled from the cell by ACA8-CML8, and calcium ion levels return to the resting state.

Stress-related lipid oxygenation, whether enzymatic or non-enzymatic, will produce compounds with multiple molecular weights. However, the common feature of many of these compounds is the existence of highly conserved carbonyl groups in the molecule. There is a large subgroup of lipid oxidation products including α，β- unsaturated carbonyl. This kind of substance is also called reactive electrophile species (RES). Naturally occurring in plants α, β-unsaturated carbonyl compounds: evk, is an active small molecule released by plants under stress[19]. Through research, this paper proposes a framework that evk, as a RES substance, can achieve plant's 'REScue' through complete defense response. The complete defense pathway is as follows: (1) recognition of evk (recognized by plant membrane protein RBOH); (2) Signal transduction (early

bioRxiv preprint doi: https://doi.org/10.1101/2023.01.24.525215; this version posted January 24, 2023. The copyright holder for this preprint (which was not certified by peer review) is the author/funder. All rights reserved. No reuse allowed without permission.

signal generation: ROS burst, intracellular calcium concentration rise and intracellular calcium concentration recovery); (3) Expression of defense genes (positive regulation of PR1 gene by WRKY53 and TGA5, up-regulation of PDF1.2 gene); (4) accumulation of active substances (accumulation of hormone JA and SA in plants). When plants are faced with various kinds of stress, they will release a lot of volatiles. Little is known about the study of volatiles. This paper provides a valuable research idea for the study of other volatiles.

Evk-mediated 'REScue' helps to promote the survival of plants. In the early stage of defense, it can achieve the resistance to biotrophic pathogens represented by SA, and in the late stage of defense, it can achieve the resistance to herbivorous insects or necrotrophic pathogens by JA, thus improving the resistance of plants and promoting plant survival. In the future, it can be used as a potential green anti-insect and anti-bacterial drug released by pure natural plants to replace highly toxic synthetic drugs.

Acknowledgments: This research was supported by the National Natural Science Foundation of China (31270655). We thank Meiqin Liu (Analysis and Testing Center, Beijing Forestry University) for her guidance on laser scanning confocal microscopy; Prof. Daoxin Xie (Tsinghua-Peking Joint Center for Life Sciences and MOE Key Laboratory of Bioinformatics, School of Life Sciences, Tsinghua University) for providing the plasmids: Cluc, Nluc pGreenII 0800-LUC and pGreenII 62-SK. All authors have approved the manuscript for publication, and no conflicts of interest exist.

Conflicts of Interest: The authors declare no conflict of interest.

Author Contributions: Design of research: J.G.and Y.S. Performed experiments: J.G., Z.G., Z.W. and L.Y. Analysed data: J.G., S. M., C.Z., S.L.Wrote the manuscript: J.G. All authors have read and agreed to the published version of the manuscript. J.G., Z.G. and Z.W. contributed equally to this work.

Data Availability Statement: The data that support the findings of this study are available from the corresponding author upon request.

References

1. Yao R, Chen L, Xie D. Irreversible strigolactone recognition: a non-canonical mechanism for hormone perception[J]. Current opinion in plant biology, 2018, 45:155-161.
2. Sheard Laura B,Tan Xu,Mao Haibin,Withers John,Ben-Nissan Gili,Hinds Thomas R,Kobayashi Yuichi,Hsu Fong-Fu,Sharon Michal,Browse John,He Sheng Yang,Rizo Josep,Howe Gregg A,Zheng Ning. Jasmonate perception by inositol-phosphate-potentiated COI1-JAZ co-receptor.[J]. Nature,2010,468(7322).
3. Farmer, E.E. Surface-to-air signals. Nature 2001, 411, 854–856.
4. Farmer, E.E.; Davoine, C. Reactive electrophile species. Curr. Opin. Plant Biol. 2007, 10, 380-386.
5. Matsui, K.; Koeduka, T. Green Leaf Volatiles in Plant Signaling and Response. Sub-Cell. Biochem. 2016, 86, 427-443.

bioRxiv preprint doi: https://doi.org/10.1101/2023.01.24.525215; this version posted January 24, 2023. The copyright holder for this preprint (which was not certified by peer review) is the author/funder. All rights reserved. No reuse allowed without permission.

6. Farmer E E, Mueller M J. ROS-Mediated Lipid Peroxidation and RES-Activated Signaling[J]. Annual Review of Plant Biology, 2013, 64(1).
7. Haridas V, Hanausek M, Nishimura G, Soehnge H, Gaikwad A, et al. 2004. Triterpenoid electrophiles (avicins) activate the innate stress response by redox regulation of a gene battery. J. Clin. Investig. 113:65-73.
8. Esterbauer H, Schaur RJ, Zollner H. 1991. Chemistry and biochemistry of 4-hydroxynonenal, malonaldehyde and related aldehydes. Free Radic. Biol. Med. 11:81-128.
9. Schmid-Siegert, E.; Loscos, J.; Farmer, E.E. Inducible malondialdehyde pools in zones of cell proliferation and developing tissues in Arabidopsis. J. Biol. Chem. 2012, 287, 8954-8962.
10. Paré, P.W.; Tumlinson, J.H. De novo biosynthesis of volatiles induced by insect herbivory in cotton plants. Plant Physiol. 1997, 114, 1161 – 1167.
11. Heiden, A.C.; Kobel, K.; Langebartels, C.; Schuh-Thomas, G.; Wildt, J. Emissions of oxygenated volatile organic compounds from plants part I: Emissions from lipoxygenase activity. J. Atmos. Chem. 2003, 45, 143-172.
12. Shiojiri, K.; Ozawa, R.; Matsui, K.; Kishimoto, K.; Kugimiya, S.; Takabayashi, J. Role of the lipoxygenase/lyase pathway of host-food plants in the host searching behavior of two parasitoid species, Cotesia glomerata and Cotesia plutellae. J. Chem. Ecol. 2006, 32, 969 – 979.
13. Alméras E, Stolz S, Vollenweider S, Reymond P, M`ene-Saffran´e L, Farmer EE. 2003. Reactive electrophile species activate defense gene expression in Arabidopsis. Plant J. 34:205 – 16.
14. Kai H, Hirashima K, Matsuda O, Ikegami H, Winkelmann T, et al. 2012. Thermotolerant cyclamen with reduced acrolein and methyl vinyl ketone. J. Exp. Bot. 63:4143 – 50
15. Mueller, S.; Hilbert, B.; Dueckershoff, K.; Roitsch, T.; Krischke, M.; Mueller, M.J.; Berger, S. General detoxification and stress responses are mediated by oxidized lipids through TGA transcription factors in Arabidopsis. Plant Cell 2008, 20, 768–785.
16. Stintzi, A.; Weber, H.; Reymond, P.; Browse, J.; Farmer, E.E. Plant defense in the absence of jasmonic acid: The role of cyclopentenones. Proc. Natl. Acad. Sci. USA 2001, 98, 12837–12842.
17. Taki, N.; Sasaki-Sekimoto, Y.; Obayashi, T.; Kikuta, A.; Kobayashi, K.; Ainai, T.; Yagi, K.; Sakurai, N.; Suzuki, H.; Masuda, T.; et al. 12-oxo-phytodienoic acid triggers expression of a distinct set of genes and plays a role in wound-induced gene expression in Arabidopsis. Plant Physiol. 2005, 139, 1268–1283.
18. Mattick, L.R.; Hand, D.B. Identification of a volatile component in soybeans that contributes to the raw bean flavor. J. Agric. Food Chem. 1969, 17, 15–17.
19. Van Poecke, R.M.P.; Posthumus, M.A.; Dicke, M. Herbivore-induced volatile production by Arabidopsis thaliana leads to attraction of the parasitoid Cotesia rubecula: Chemical, behavioral, and gene-expression analysis. J. Chem. Ecol. 2001, 27, 1911–1928.
20. Salch, Y.P.; Grove, M.J.; Takamura, H.; Gardner, H.W. Characterization of a C-5,13-Cleaving Enzyme of 13(S)-Hydroperoxide of Linolenic Acid by Soybean Seed. Plant Physiol. 1995, 108, 1211–1218.
21. Fishera, A.J.; Grimesb, H.D.; Fall, R. The biochemical origin of pentenol emissions from wounded leaves. Phytochemistry 2003, 62, 159–163.

bioRxiv preprint doi: https://doi.org/10.1101/2023.01.24.525215; this version posted January 24, 2023. The copyright holder for this preprint (which was not certified by peer review) is the author/funder. All rights reserved. No reuse allowed without permission.

22. Meucci, A.; Shiriaev, A.; Rosellini, I.; Malorgio, F.; Pezzarossa, B. Se-Enrichment Pattern, Composition, and Aroma Profile of Ripe Tomatoes after Sodium Selenate Foliar Spraying Performed at Different Plant Developmental Stages. Plants 2021, 10, 1050.
23. Gong J.Q.; Yao L. J.; Jiao C. Y.; Guo Z. J.; Li S. W.; Zuo Y. X.; Shen Y. B. Ethyl Vinyl Ketone Activates K+ Efflux to Regulate Stomatal Closure by MRP4-Dependent eATP Accumulation Working Upstream of H2O2 Burst in Arabidopsis[J]. International Journal of Molecular Sciences,2022,23(16).
24. Kiep, V.; Vadassery, J.; Lattke, J.; Maaß, J.; Boland, W.; Peiter, E.; Mithöfer, A. Systemic cytosolic Ca2+ elevation is activated upon wounding and herbivory in Arabidopsis. New Phytol. 2015, 207, 996–1004.
25. Ranf, S.; Eschen-Lippold, L.; Pecher, P.; Lee, J.; Scheel, D. Interplay between calcium signalling and early signalling elements during defence responses to microbe- or damage-associated molecular patterns. Plant J. 2011, 68, 100–113.
26. Kudla, J.; Batistic, O.; Hashimoto, K. Calcium Signals: The Lead Currency of Plant Information Processing. Plant Cell 2010, 22, 541-563.
27. Kawarazaki T , Kimura S , Iizuka A , et al. A low temperature-inducible protein AtSRC2 enhances the ROS-producing activity of NADPH oxidase AtRbohF[J]. Biochimica Et Biophysica Acta, 2013, 1833(12):2775-2780.
28. Choi J, Tanaka K, Cao Y， et al. Identification of a Plant Receptor for Extracellular ATP[J]. Science, 343, 290–294 . 2014
29. Gilroy, S.; Suzuki, N.; Miller, G.; Choi, W.; Toyota, M.; Devireddy, A.R.; Mittler, R. A tidal wave of signals: Calcium and ROS at the forefront of rapid systemic signaling. Trends Plant Sci. 2014, 19, 623–630.
30. Du L, Chen Z. Identification of genes encoding receptor‐like protein kinases as possible targets of pathogen‐and salicylic acid‐induced WRKY DNA‐binding proteins in Arabidopsis. Plant J. 2000, 24(6): 837-847
31. Dong J, Chen C, Chen Z, Expression profiles of the Arabidopsis WRKY gene superfamily during plant defense response. Plant Mol Biol. 2002, 51: 21-37
32. Pandey SP, Somssich IE. The role of WRKY transcription factors in plant immunity. Plant Physiology 2009, 150(4): 1648-1655
33. Rushton PJ, Somssich IE, Ringler P, Shen QJ. WRKY transcription factors. Trends in Plant Science 2010, 15(5): 247-258
34. Jiang Y, Liang G, Yu D. Activated expression of WRKY57 confers drought tolerance in Arabidopsis. Mol Plant. 2012, 5(6): 1375-1388
35. Ding ZJ, Yan JY, Xu XY, Li GX, Zheng SJ. WRKY46 functions as a transcriptional repressor of ALMT1, regulating aluminum-induced malate secretion in Arabidopsis. Plant J. 2013, 76(5): 825-835
36. Murray S L , Ingle R A , Petersen L N , et al. Basal resistance against Pseudomonas syringae in Arabidopsis involves WRKY53 and a protein with homology to a nematode resistance protein.[J]. Mol Plant Microbe Interact, 2007, 20(11):1431-1438.
37. Miao Y , Laun T , Zimmermann P , et al. Targets of the WRKY53 transcription factor and its role during leaf senescence in Arabidopsis[J]. Plant Molecular Biology, 2004, 55(6):853-867.
38. Miao, Y.; Laun, T.M.; Smykowski, A.; Zentgraf, U. Arabidopsis MEKK1 can take a short cut: It can directly interact with senescence-related WRKY53 transcription factor on the protein

bioRxiv preprint doi: https://doi.org/10.1101/2023.01.24.525215; this version posted January 24, 2023. The copyright holder for this preprint (which was not certified by peer review) is the author/funder. All rights reserved. No reuse allowed without permission.

level and can bind to its promoter. Plant Mol. Biol. 2007, 65, 63–76. [CrossRef]

39. Miao, Y.; Smykowski, A.; Zentgraf, U. A novel upstream regulator of WRKY53 transcription during leaf senescence in Arabidopsis thaliana. Plant Biol. 2008, 10 (Suppl. 1), 110–120.
40. Sun, YD, DQ. Activated expression of AtWRKY53 negatively regulates drought tolerance by mediating stomatal movement[J]. PLANT CELL REP, 2015, 2015,34(8)(-):1295-1306.
41. Yan, C.; Fan, M.; Yang, M.; Zhao, J.; Zhang, W.; Su, Y.; Xiao, L.; Deng, H.; Xie, D. Injury Activates Ca2+/Calmodulin-Dependent Phosphorylation of JAV1-JAZ8-WRKY51 Complex for Jasmonate Biosynthesis. Mol. Cell 2018, 70, 136–149.e7.Petersen et al., 2000
42. Bouche N, Yellin A, Snedden, WA, Fromm H. Plant-specific calmodulin-binding proteins. Annu. Rev. Plant Biol. 2005, 56: 435-466
43. Yang T, Poovaiah BW. Calcium/calmodulin-mediated signal network in plants. Trends Plant Sci. 2003, 8: 505-512
44. Snedden, WA, Fromm H. Calmodulin as a versatile calcium signal transducer in plants. New Phytol. 2001, 151: 35-66
45. Kim MC, Chung WS, Yun DJ, Cho MJ. Calcium and calmodulin-mediated regulation of gene expression in plants. Molecular Plant 2009, 2(1): 13-21
46. Wasternack C , Forner S , Strnad M , et al. Jasmonates in flower and seed development[J]. Biochimie, 2013, 95(1):79-85.
47. Stotz Henrik U, Jikumaru Yusuke, Shimada Yukihisa, 等. Jasmonate-Dependent and COI1-Independent Defense Responses Against Sclerotinia sclerotiorum in Arabidopsis thaliana: Auxin is Part of COI1-Independent Defense Signaling[J]. Plant & Cell Physiology, 2011(11):11.
48. Biswas M S , Mano J ' I . Lipid Peroxide-Derived Short-Chain Carbonyls Mediate Hydrogen Peroxide-Induced and Salt-Induced Programmed Cell Death in Plants 1[OPEN][J]. Plant physiology, 2015, 168(3):885-898.
49. Findling S , Stotz H U , Zoeller M , et al. TGA2 signaling in response to reactive electrophile species is not dependent on cysteine modification of TGA2[J]. PLoS ONE, 2018, 13(4).
50. Mueller M J , Berger S . Reactive electrophilic oxylipins: Pattern recognition and signalling[J]. Phytochemistry, 2009, 70(13-14):1511-1521.
51. Stefan, Mueller, Beate, et al. General Detoxification and Stress Responses Are Mediated by Oxidized Lipids through TGA Transcription Factors in Arabidopsis[J]. The Plant Cell, 2008.
52. Chengbin Xiang, Z H Miao, Eric Lam. Coordinated activation of as-1-type elements and a tobacco glutathione S-transferase gene by auxins, salicylic acid, methyl-jasmonate and hydrogen peroxide[J]. Plant Molecular Biology, 1996, 32(3):415-426.
53. Pascuzzi P , Hamilton D , Bodily K , et al. Auxin-induced Stress Potentiates trans-activation by a Conserved Plant Basic/Leucine-zipper Factor[J]. Journal of Biological Chemistry, 1998, 273(41):26631-26637.
54. Chen W , Singh K B . The auxin, hydrogen peroxide and salicylic acid induced expression of the Arabidopsis GST6 promoter is mediated in part by an ocs element[J]. The Plant Journal, 1999, 19(6):667-677.
55. K. JöhnkD. Straile. Xenobiotic- and jasmonic acid-inducible signal transduction pathways have become interdependent at the Arabidopsis CYP81D11 promoter.[J]. Plant Physiology, 2012, 159(3):1292-1292.
56. Zhang Y , Fan W , Kinkema M , et al. Interaction of NPR1 with Basic Leucine Zipper Protein

bioRxiv preprint doi: https://doi.org/10.1101/2023.01.24.525215; this version posted January 24, 2023. The copyright holder for this preprint (which was not certified by peer review) is the author/funder. All rights reserved. No reuse allowed without permission.

951 Transcription Factors That Bind Sequences Required for Salicylic Acid Induction of the PR-1
952 Gene[J]. Proceedings of the National Academy of Sciences of the United States of America,
953 1999, 96(11):6523-6528.
954 57. J.-Ma. Zhou, Youssef Trifa, Herman Silva,等. NPR1 Differentially Interacts with Members of
955 the TGA/OBF Family of Transcription Factors That Bind an Element of the PR-1 Gene
956 Required for Induction by Salicylic Acid[J]. Molecular Plant-Microbe Interactions, 2000,
957 13(2):191-202.
958 58. Fan W , Dong X . In Vivo Interaction between NPR1 and Transcription Factor TGA2 Leads
959 to Salicylic Acid-Mediated Gene Activation in Arabidopsis[J]. Plant Cell, 2002,
960 14(6):1377-1389.
961 59. Gatz C (2013) From pioneers to team players: TGA transcription factors provide a molecular
962 link between diferent stress pathways. Mol Plant Microbe Interact 26:151–159
963 60. Hussain RMF (2012) WRKY transcription factors involved in PR-1 gene expression in
964 Arabidopsis. Doctoral thesis, Leiden University
965 61. Kesarwani M, Yoo J, Dong X (2007) Genetic interactions of TGA transcription factors in the
966 regulation of pathogenesis-related genes and disease resistance in Arabidopsis. Plant Physiol
967 144:336–346
968 62. Johnson C, Boden E, Arias J (2003) Salicylic acid and NPR1 induce the recruitment of
969 trans-activating TGA factors to a defense gene promoter in Arabidopsis. Plant Cell 15:1846–
970 1858
971 63. Wu, J. X.; Liu, R.; Song, K.; Chen, L. Structures of human dual oxidase 1 complex in
972 low-calcium and high-calcium states. Nat Commun 2021, 12, 155.
973 64. Magnani, F.; Nenci, S.; Millana Fananas, E.; Ceccon, M.; Romero, E.; Fraaije, M. W.;
974 Mattevi, A. Crystal structures and atomic model of NADPH oxidase. Proceedings of the
975 National Academy of Sciences 2017, 114, 6764-6769.
976 65. Bokoch, G. M.; Knaus, U. G. NADPH oxidases: not just for leukocytes anymore! Trends
977 Biochem Sci 2003, 28, 502-508.
978 66. Arimura G, Ozawa R, Shimoda T, Nishioka T, Boland W, Takabayashi J. Herbivory-induced
979 volatiles elicit defence genes in lima bean leaves. Nature 2000; 406: 512-5.
980 67. Takabayashi J, Dicke M. Plant-carnivore mutualism through herbivore-induced carnivore
981 attractants. Trends Plant Sci 1996; 1: 109-13.
982 68. Van Poecke, R.M.P.; Posthumus, M.A.; Dicke, M. Herbivore-induced volatile production by
983 Arabidopsis thaliana leads to attraction of the parasitoid Cotesia rubecula: Chemical,
984 behavioral, and gene-expression analysis. J. Chem. Ecol. 2001, 27, 1911–1928.
985 69. Gong, J.; Yao, L.; Jiao, C.; Guo, Z.; Li, S.; Zuo, Y.; Shen, Y. Ethyl Vinyl Ketone Activates K+
986 Efflflux to Regulate Stomatal Closure by MRP4-Dependent eATP Accumulation Working
987 Upstream of H2O2 Burst in Arabidopsis. Int. J. Mol. Sci. 2022, 23, 9002.
988 70. S. Conn, M. Gilliham, Comparative physiology of elemental distributions in plants, Ann. Bot.
989 105 (2010) 1081e1102.
990 71. H. Nomura, R. Shiina, Calcium signaling in plant endosymbiotic organelles: mechanism and
991 role in physiology, Mol. Plant 7 (2014) 1094e1104.
992 72. Jiao, C.; Gong, J.; Guo, Z.; Li, S.; Zuo, Y.; Shen, Y. Linalool Activates Oxidative and
993 Calcium Burst and CAM3-ACA8 Participates in Calcium Recovery in Arabidopsis Leaves.
994 Int. J. Mol. Sci. 2022, 23, 5357.

bioRxiv preprint doi: https://doi.org/10.1101/2023.01.24.525215; this version posted January 24, 2023. The copyright holder for this preprint (which was not certified by peer review) is the author/funder. All rights reserved. No reuse allowed without permission.

73. Asai, N.; Nishioka, T.; Takabayashi, J.; Furuichi, T. Plant volatiles regulate the activities of Ca2+-permeable channels and promote cytoplasmic calcium transients in Arabidopsis leaf cells. Plant Signal. Behav. 2009, 4, 294 – 300.
74. Huda, K.M.K.; Banu, M.S.A.; Tuteja, B.; Tuteja, N. Global calcium transducer P-type Ca-ATPases open new avenues for agriculture by regulating stress signalling. J. Exp. Bot. 2013, 64, 3099 – 3109.
75. Zheng, X.Y., Spivey, N.W., Zeng, W., Liu, P.P., Fu, Z.Q., Klessig, D.F., He, S.Y., and Dong, X. (2012). Coronatine promotes Pseudomonas syringae virulence in plants by activating a signaling cascade that inhibits salicylic acid accumulation. Cell Host Microbe 11, 587 – 596.
76. Spoel, S.H., and Dong, X. (2008). Making sense of hormone crosstalk during plant immune responses. Cell Host Microbe 3, 348 – 351.
77. Laurie-Berry, N., Joardar, V., Street, I.H., and Kunkel, B.N. (2006). The Arabidopsis thaliana JASMONATE INSENSITIVE 1 gene is required for suppression of salicylic acid-dependent defenses during infection by Pseudomonas syringae. Mol. Plant Microbe Interact. 19, 789 – 800.
78. Laudert, D., and Weiler, E.W. (1998). Allene oxide synthase: a major control point in Arabidopsis thaliana octadecanoid signalling. Plant J. 15, 675 – 684.
79. Spoel, S.H., Koornneef, A., Claessens, S.M., Korzelius, J.P., Van Pelt, J.A., Mueller, M.J., Buchala, A.J., Me´traux, J.P., Brown, R., Kazan, K., et al. (2003). NPR1 modulates cross-talk between salicylate- and jasmonatedependent defense pathways through a novel function in the cytosol. Plant Cell 15, 760 – 770.
80. Van der Does, D., Leon-Reyes, A., Koornneef, A., Van Verk, M.C., Rodenburg, N., Pauwels, L., Goossens, A., Ko¨ rbes, A.P., Memelink, J., Ritsema, T., et al. (2013). Salicylic acid suppresses jasmonic acid signaling downstream of SCFCOI1-JAZ by targeting GCC promoter motifs via transcription factor ORA59. Plant Cell 25, 744–761.
81. Hong-Mei Yuan,Wen-Cheng Liu,Ying-Tang Lu. CATALASE2 Coordinates SA-Mediated Repression of Both Auxin Accumulation and JA Biosynthesis in Plant Defenses[J]. Cell Host & Microbe,2017,21(2).

Acknowledgments: This research was supported by the National Natural Science Foundation of China (31270655). We thank Meiqin Liu (Analysis and Testing Center, Beijing Forestry University) for her guidance on laser scanning confocal microscopy; Prof. Daoxin Xie (Tsinghua-Peking Joint Center for Life Sciences and MOE Key Laboratory of Bioinformatics, School of Life Sciences, Tsinghua University) for providing the plasmids: Cluc, Nluc pGreenII 0800-LUC and pGreenII 62-SK. All authors have approved the manuscript for publication, and no conflicts of interest exist.

Author Contributions: Design of research: J.G.and Y.S.Performed experiments: J.G., Z. G. and Z. W. L.Y. Analysed data: J.G., S. M., C.Z., S.L.Wrote the manuscript: J.G. All authors have read and agreed to the published version of the manuscript. J.G., Z.G. and Z.W. contributed equally to this work.

Conflicts of Interest: The authors declare no conflicts of interest.

bioRxiv preprint doi: https://doi.org/10.1101/2023.01.24.525215; this version posted January 24, 2023. The copyright holder for this preprint (which was not certified by peer review) is the author/funder. All rights reserved. No reuse allowed without permission.

1039

1040

bioRxiv preprint doi: https://doi.org/10.1101/2023.01.24.525215; this version posted January 24, 2023. The copyright holder for this preprint (which was not certified by peer review) is the author/funder. All rights reserved. No reuse allowed without permission.

Parsed Citations

Yao R, Chen L, Xie D. Irreversible strigolactone recognition: a non-canonical mechanism for hormone perception[J]. Current opinion in plant biology, 2018, 45:155-161.
Google Scholar: Author Only Title Only Author and Title

Sheard Laura B,Tan Xu,Mao Haibin,Withers John,Ben-Nissan Gili,Hinds Thomas R,Kobayashi Yuichi,Hsu Fong-Fu,Sharon Michal,Browse John,He Sheng Yang,Rizo Josep,Howe Gregg A,Zheng Ning. Jasmonate perception by inositol-phosphate-potentiated COI1-JAZ co-receptor.[J]. Nature,2010,468(7322).

Farmer, E.E. Surface-to-air signals. Nature 2001, 411, 854–856.
Google Scholar: Author Only Title Only Author and Title

Farmer, E.E.; Davoine, C. Reactive electrophile species. Curr. Opin. Plant Biol. 2007, 10, 380-386.
Google Scholar: Author Only Title Only Author and Title

Matsui, K.; Koeduka, T. Green Leaf Volatiles in Plant Signaling and Response. Sub-Cell. Biochem. 2016, 86, 427-443.
Google Scholar: Author Only Title Only Author and Title

Farmer E E, Mueller M J. ROS-Mediated Lipid Peroxidation and RES-Activated Signaling[J]. Annual Review of Plant Biology, 2013, 64(1).

Haridas V, Hanausek M, Nishimura G, Soehnge H, Gaikwad A, et al. 2004. Triterpenoid electrophiles (avicins) activate the innate stress response by redox regulation of a gene battery. J. Clin. Investig. 113:65-73.
Google Scholar: Author Only Title Only Author and Title

Esterbauer H, Schaur RJ, Zollner H. 1991. Chemistry and biochemistry of 4-hydroxynonenal, malonaldehyde and related aldehydes. Free Radic. Biol. Med. 11:81-128.
Google Scholar: Author Only Title Only Author and Title

Schmid-Siegert, E.; Loscos, J.; Farmer, E.E. Inducible malondialdehyde pools in zones of cell proliferation and developing tissues in Arabidopsis. J. Biol. Chem. 2012, 287, 8954-8962.
Google Scholar: Author Only Title Only Author and Title

Paré, P.W.; Tumlinson, J.H. De novo biosynthesis of volatiles induced by insect herbivory in cotton plants. Plant Physiol. 1997, 114, 1161–1167.
Google Scholar: Author Only Title Only Author and Title

Heiden, A.C.; Kobel, K.; Langebartels, C.; Schuh-Thomas, G.; Wildt, J. Emissions of oxygenated volatile organic compounds from plants part I: Emissions from lipoxygenase activity. J. Atmos. Chem. 2003, 45, 143-172.
Google Scholar: Author Only Title Only Author and Title

Shiojiri, K.; Ozawa, R.; Matsui, K.; Kishimoto, K.; Kugimiya, S.; Takabayashi, J. Role of the lipoxygenase/lyase pathway of host-food plants in the host searching behavior of two parasitoid species, Cotesia glomerata and Cotesia plutellae. J. Chem. Ecol. 2006, 32, 969–979.
Google Scholar: Author Only Title Only Author and Title

Alméras E, Stolz S, Vollenweider S, Reymond P, M`ene-Saffran´e L, Farmer EE. 2003. Reactive electrophile species activate defense gene expression in Arabidopsis. Plant J. 34:205–16.
Google Scholar: Author Only Title Only Author and Title

Kai H, Hirashima K, Matsuda O, Ikegami H, Winkelmann T, et al. 2012. Thermotolerant cyclamen with reduced acrolein and methyl vinyl ketone. J. Exp. Bot. 63:4143–50
Google Scholar: Author Only Title Only Author and Title

Mueller, S.; Hilbert, B.; Dueckershoff, K.; Roitsch, T.; Krischke, M.; Mueller, M.J.; Berger, S. General detoxification and stress responses are mediated by oxidized lipids through TGA transcription factors in Arabidopsis. Plant Cell 2008, 20, 768–785.
Google Scholar: Author Only Title Only Author and Title

Stintzi, A.; Weber, H.; Reymond, P.; Browse, J.; Farmer, E.E. Plant defense in the absence of jasmonic acid: The role of cyclopentenones. Proc. Natl. Acad. Sci. USA 2001, 98, 12837–12842.
Google Scholar: Author Only Title Only Author and Title

Taki, N.; Sasaki-Sekimoto, Y.; Obayashi, T.; Kikuta, A.; Kobayashi, K.; Ainai, T.; Yagi, K.; Sakurai, N.; Suzuki, H.; Masuda, T.; et al. 12-oxo-phytodienoic acid triggers expression of a distinct set of genes and plays a role in wound-induced gene expression in Arabidopsis. Plant Physiol. 2005, 139, 1268–1283.
Google Scholar: Author Only Title Only Author and Title

Mattick, L.R.; Hand, D.B. Identification of a volatile component in soybeans that contributes to the raw bean flavor. J. Agric. Food Chem. 1969, 17, 15–17.

bioRxiv preprint doi: https://doi.org/10.1101/2023.01.24.525215; this version posted January 24, 2023. The copyright holder for this preprint (which was not certified by peer review) is the author/funder. All rights reserved. No reuse allowed without permission.

Google Scholar: Author Only Title Only Author and Title

Van Poecke, R.M.P.; Posthumus, M.A.; Dicke, M. Herbivore-induced volatile production by Arabidopsis thaliana leads to attraction of the parasitoid Cotesia rubecula: Chemical, behavioral, and gene-expression analysis. J. Chem. Ecol. 2001, 27, 1911–1928.
Google Scholar: Author Only Title Only Author and Title

Salch, Y.P.; Grove, M.J.; Takamura, H.; Gardner, H.W. Characterization of a C-5,13-Cleaving Enzyme of 13(S)-Hydroperoxide of Linolenic Acid by Soybean Seed. Plant Physiol. 1995, 108, 1211–1218.
Google Scholar: Author Only Title Only Author and Title

Fishera, A.J.; Grimesb, H.D.; Fall, R. The biochemical origin of pentenol emissions from wounded leaves. Phytochemistry 2003, 62, 159–163.
Google Scholar: Author Only Title Only Author and Title

Meucci, A.; Shiriaev, A.; Rosellini, I.; Malorgio, F.; Pezzarossa, B. Se-Enrichment Pattern, Composition, and Aroma Profile of Ripe Tomatoes after Sodium Selenate Foliar Spraying Performed at Different Plant Developmental Stages. Plants 2021, 10, 1050.
Google Scholar: Author Only Title Only Author and Title

Gong J.Q.; Yao L. J.; Jiao C. Y.; Guo Z. J.; Li S. W.; Zuo Y. X.; Shen Y. B. Ethyl Vinyl Ketone Activates K+ Efflux to Regulate Stomatal Closure by MRP4-Dependent eATP Accumulation Working Upstream of H2O2 Burst in Arabidopsis[J]. International Journal of Molecular Sciences,2022,23(16).

Kiep, V.; Vadassery, J.; Lattke, J.; Maaß, J.; Boland, W.; Peiter, E.; Mithöfer, A. Systemic cytosolic Ca2+ elevation is activated upon wounding and herbivory in Arabidopsis. New Phytol. 2015, 207, 996–1004.
Google Scholar: Author Only Title Only Author and Title

Ranf, S.; Eschen-Lippold, L.; Pecher, P.; Lee, J.; Scheel, D. Interplay between calcium signalling and early signalling elements during defence responses to microbe- or damage-associated molecular patterns. Plant J. 2011, 68, 100–113.
Google Scholar: Author Only Title Only Author and Title

Kudla, J.; Batistic, O.; Hashimoto, K. Calcium Signals: The Lead Currency of Plant Information Processing. Plant Cell 2010, 22, 541-563.
Google Scholar: Author Only Title Only Author and Title

Kawarazaki T , Kimura S , Iizuka A , et al. A low temperature-inducible protein AtSRC2 enhances the ROS-producing activity of NADPH oxidase AtRbohF[J]. Biochimica Et Biophysica Acta, 2013, 1833(12):2775-2780.
Google Scholar: Author Only Title Only Author and Title

Choi J, Tanaka K, Cao Y, et al. Identification of a Plant Receptor for Extracellular ATP[J]. Science, 343, 290–294 . 2014
Google Scholar: Author Only Title Only Author and Title

Gilroy, S.; Suzuki, N.; Miller, G.; Choi, W.; Toyota, M.; Devireddy, A.R.; Mittler, R. A tidal wave of signals: Calcium and ROS at the forefront of rapid systemic signaling. Trends Plant Sci. 2014, 19, 623–630.
Google Scholar: Author Only Title Only Author and Title

Du L, Chen Z. Identification of genes encoding receptor-like protein kinases as possible targets of pathogen-and salicylic acid-induced WRKY DNA-binding proteins in Arabidopsis. Plant J. 2000, 24(6): 837-847
Google Scholar: Author Only Title Only Author and Title

Dong J, Chen C, Chen Z, Expression profiles of the Arabidopsis WRKY gene superfamily during plant defense response. Plant Mol Biol. 2002, 51: 21-37
Google Scholar: Author Only Title Only Author and Title

Pandey SP, Somssich IE. The role of WRKY transcription factors in plant immunity. Plant Physiology 2009, 150(4): 1648-1655
Google Scholar: Author Only Title Only Author and Title

Rushton PJ, Somssich IE, Ringler P, Shen QJ. WRKY transcription factors. Trends in Plant Science 2010, 15(5): 247-258
Google Scholar: Author Only Title Only Author and Title

Jiang Y, Liang G, Yu D. Activated expression of WRKY57 confers drought tolerance in Arabidopsis. Mol Plant. 2012, 5(6): 1375-1388
Google Scholar: Author Only Title Only Author and Title

Ding ZJ, Yan JY, Xu XY, Li GX, Zheng SJ. WRKY46 functions as a transcriptional repressor of ALMT1, regulating aluminum-induced malate secretion in Arabidopsis. Plant J. 2013, 76(5): 825-835
Google Scholar: Author Only Title Only Author and Title

Murray S L , Ingle R A , Petersen L N , et al. Basal resistance against Pseudomonas syringae in Arabidopsis involves WRKY53 and a protein with homology to a nematode resistance protein.[J]. Mol Plant Microbe Interact, 2007, 20(11):1431-1438.
Google Scholar: Author Only Title Only Author and Title

bioRxiv preprint doi: https://doi.org/10.1101/2023.01.24.525215; this version posted January 24, 2023. The copyright holder for this preprint (which was not certified by peer review) is the author/funder. All rights reserved. No reuse allowed without permission.

Miao Y , Laun T , Zimmermann P , et al. Targets of the WRKY53 transcription factor and its role during leaf senescence in Arabidopsis[J]. Plant Molecular Biology, 2004, 55(6):853-867.
Google Scholar: Author Only Title Only Author and Title

Miao, Y.; Laun, T.M.; Smykowski, A; Zentgraf, U. Arabidopsis MEKK1 can take a short cut: It can directly interact with senescence-related WRKY53 transcription factor on the protein level and can bind to its promoter. Plant Mol. Biol. 2007, 65, 63–76. [CrossRef]
Google Scholar: Author Only Title Only Author and Title

Miao, Y.; Smykowski, A; Zentgraf, U. A novel upstream regulator of WRKY53 transcription during leaf senescence in Arabidopsis thaliana. Plant Biol. 2008, 10 (Suppl. 1), 110–120.
Google Scholar: Author Only Title Only Author and Title

Sun, YD, DQ. Activated expression of AtWRKY53 negatively regulates drought tolerance by mediating stomatal movement[J]. PLANT CELL REP, 2015, 2015,34(8)(-):1295-1306.
Google Scholar: Author Only Title Only Author and Title

Yan, C.; Fan, M.; Yang, M.; Zhao, J.; Zhang, W.; Su, Y.; Xiao, L.; Deng, H.; Xie, D. Injury Activates Ca2+/Calmodulin-Dependent Phosphorylation of JAV1-JAZ8-WRKY51 Complex for Jasmonate Biosynthesis. Mol. Cell 2018, 70, 136–149.e7.Petersen et al., 2000
Google Scholar: Author Only Title Only Author and Title

Bouche N, Yellin A, Snedden, WA, Fromm H. Plant-specific calmodulin-binding proteins. Annu. Rev. Plant Biol. 2005, 56: 435-466
Google Scholar: Author Only Title Only Author and Title

Yang T, Poovaiah BW. Calcium/calmodulin-mediated signal network in plants. Trends Plant Sci. 2003, 8: 505-512
Google Scholar: Author Only Title Only Author and Title

Snedden, WA, Fromm H. Calmodulin as a versatile calcium signal transducer in plants. New Phytol. 2001, 151: 35-66
Google Scholar: Author Only Title Only Author and Title

Kim MC, Chung WS, Yun DJ, Cho MJ. Calcium and calmodulin-mediated regulation of gene expression in plants. Molecular Plant 2009, 2(1): 13-21
Google Scholar: Author Only Title Only Author and Title

Wasternack C , Forner S , Strnad M , et al. Jasmonates in flower and seed development[J]. Biochimie, 2013, 95(1):79-85.
Google Scholar: Author Only Title Only Author and Title

Stotz Henrik U, Jikumaru Yusuke, Shimada Yukihisa,等. Jasmonate-Dependent and COI1-Independent Defense Responses Against Sclerotinia sclerotiorum in Arabidopsis thaliana: Auxin is Part of COI1-Independent Defense Signaling[J]. Plant & Cell Physiology, 2011(11):11.

Biswas M S , Mano J ' I . Lipid Peroxide-Derived Short-Chain Carbonyls Mediate Hydrogen Peroxide-Induced and Salt-Induced Programmed Cell Death in Plants 1[OPEN][J]. Plant physiology, 2015, 168(3):885-898.
Google Scholar: Author Only Title Only Author and Title

Findling S , Stotz H U , Zoeller M , et al. TGA2 signaling in response to reactive electrophile species is not dependent on cysteine modification of TGA2[J]. PLoS ONE, 2018, 13(4).

Mueller M J , Berger S . Reactive electrophilic oxylipins: Pattern recognition and signalling[J]. Phytochemistry, 2009, 70(13-14):1511-1521.
Google Scholar: Author Only Title Only Author and Title

Stefan, Mueller, Beate, et al. General Detoxification and Stress Responses Are Mediated by Oxidized Lipids through TGA Transcription Factors in Arabidopsis[J]. The Plant Cell, 2008.
Google Scholar: Author Only Title Only Author and Title

Chengbin Xiang, Z H Miao, Eric Lam. Coordinated activation of as-1-type elements and a tobacco glutathione S-transferase gene by auxins, salicylic acid, methyl-jasmonate and hydrogen peroxide[J]. Plant Molecular Biology, 1996, 32(3):415-426.
Google Scholar: Author Only Title Only Author and Title

Pascuzzi P , Hamilton D , Bodily K , et al. Auxin-induced Stress Potentiates trans-activation by a Conserved Plant Basic/Leucine-zipper Factor[J]. Journal of Biological Chemistry, 1998, 273(41):26631-26637.
Google Scholar: Author Only Title Only Author and Title

Chen W , Singh K B . The auxin, hydrogen peroxide and salicylic acid induced expression of the Arabidopsis GST6 promoter is mediated in part by an ocs element[J]. The Plant Journal, 1999, 19(6):667-677.
Google Scholar: Author Only Title Only Author and Title

K. JöhnkD. Straile. Xenobiotic- and jasmonic acid-inducible signal transduction pathways have become interdependent at the Arabidopsis CYP81D11 promoter.[J]. Plant Physiology, 2012, 159(3):1292-1292.
Google Scholar: Author Only Title Only Author and Title

bioRxiv preprint doi: https://doi.org/10.1101/2023.01.24.525215; this version posted January 24, 2023. The copyright holder for this preprint (which was not certified by peer review) is the author/funder. All rights reserved. No reuse allowed without permission.

Zhang Y , Fan W , Kinkema M , et al. Interaction of NPR1 with Basic Leucine Zipper Protein Transcription Factors That Bind Sequences Required for Salicylic Acid Induction of the PR-1 Gene[J]. Proceedings of the National Academy of Sciences of the United States of America, 1999, 96(11):6523-6528.
Google Scholar: Author Only Title Only Author and Title

J.-Ma. Zhou, Youssef Trifa, Herman Silva,等. NPR1 Differentially Interacts with Members of the TGA/OBF Family of Transcription Factors That Bind an Element of the PR-1 Gene Required for Induction by Salicylic Acid[J]. Molecular Plant-Microbe Interactions, 2000, 13(2):191-202.
Google Scholar: Author Only Title Only Author and Title

Fan W , Dong X . In Vivo Interaction between NPR1 and Transcription Factor TGA2 Leads to Salicylic Acid-Mediated Gene Activation in Arabidopsis[J]. Plant Cell, 2002, 14(6):1377-1389.
Google Scholar: Author Only Title Only Author and Title

Gatz C (2013) From pioneers to team players: TGA transcription factors provide a molecular link between diferent stress pathways. Mol Plant Microbe Interact 26:151–159
Google Scholar: Author Only Title Only Author and Title

Hussain RMF (2012) WRKY transcription factors involved in PR-1 gene expression in Arabidopsis. Doctoral thesis, Leiden University
Google Scholar: Author Only Title Only Author and Title

Kesarwani M, Yoo J, Dong X (2007) Genetic interactions of TGA transcription factors in the regulation of pathogenesis-related genes and disease resistance in Arabidopsis. Plant Physiol 144:336–346
Google Scholar: Author Only Title Only Author and Title

Johnson C, Boden E, Arias J (2003) Salicylic acid and NPR1 induce the recruitment of trans-activating TGA factors to a defense gene promoter in Arabidopsis. Plant Cell 15:1846–1858
Google Scholar: Author Only Title Only Author and Title

Wu, J. X.; Liu, R.; Song, K.; Chen, L. Structures of human dual oxidase 1 complex in low-calcium and high-calcium states. Nat Commun 2021, 12, 155.
Google Scholar: Author Only Title Only Author and Title

Magnani, F.; Nenci, S.; Millana Fananas, E.; Ceccon, M.; Romero, E.; Fraaije, M. W.; Mattevi, A. Crystal structures and atomic model of NADPH oxidase. Proceedings of the National Academy of Sciences 2017, 114, 6764-6769.
Google Scholar: Author Only Title Only Author and Title

Bokoch, G. M.; Knaus, U. G. NADPH oxidases: not just for leukocytes anymore! Trends Biochem Sci 2003, 28, 502-508.
Google Scholar: Author Only Title Only Author and Title

Arimura G, Ozawa R, Shimoda T, Nishioka T, Boland W, Takabayashi J. Herbivory-induced volatiles elicit defence genes in lima bean leaves. Nature 2000; 406: 512-5.
Google Scholar: Author Only Title Only Author and Title

Takabayashi J, Dicke M. Plant-carnivore mutualism through herbivore-induced carnivore attractants. Trends Plant Sci 1996; 1: 109-13.
Google Scholar: Author Only Title Only Author and Title

Van Poecke, R.M.P.; Posthumus, M.A.; Dicke, M. Herbivore-induced volatile production by Arabidopsis thaliana leads to attraction of the parasitoid Cotesia rubecula: Chemical, behavioral, and gene-expression analysis. J. Chem. Ecol. 2001, 27, 1911–1928.
Google Scholar: Author Only Title Only Author and Title

Gong, J.; Yao, L.; Jiao, C.; Guo, Z.; Li, S.; Zuo, Y.; Shen, Y. Ethyl Vinyl Ketone Activates K+ Efflflux to Regulate Stomatal Closure by MRP4-Dependent eATP Accumulation Working Upstream of H2O2 Burst in Arabidopsis. Int. J. Mol. Sci. 2022, 23, 9002.
Google Scholar: Author Only Title Only Author and Title

S. Conn, M. Gilliham, Comparative physiology of elemental distributions in plants, Ann. Bot. 105 (2010) 1081e1102.
Google Scholar: Author Only Title Only Author and Title

H. Nomura, R. Shiina, Calcium signaling in plant endosymbiotic organelles: mechanism and role in physiology, Mol. Plant 7 (2014) 1094e1104.
Google Scholar: Author Only Title Only Author and Title

Jiao, C.; Gong, J.; Guo, Z.; Li, S.; Zuo, Y.; Shen, Y. Linalool Activates Oxidative and Calcium Burst and CAM3-ACA8 Participates in Calcium Recovery in Arabidopsis Leaves. Int. J. Mol. Sci. 2022, 23, 5357.
Google Scholar: Author Only Title Only Author and Title

Asai, N.; Nishioka, T.; Takabayashi, J.; Furuichi, T. Plant volatiles regulate the activities of Ca2+-permeable channels and promote cytoplasmic calcium transients in Arabidopsis leaf cells. Plant Signal. Behav. 2009, 4, 294–300.

bioRxiv preprint doi: https://doi.org/10.1101/2023.01.24.525215; this version posted January 24, 2023. The copyright holder for this preprint (which was not certified by peer review) is the author/funder. All rights reserved. No reuse allowed without permission.

Google Scholar: Author Only Title Only Author and Title

Huda, K.M.K.; Banu, M.S.A; Tuteja, B.; Tuteja, N. Global calcium transducer P-type Ca-ATPases open new avenues for agriculture by regulating stress signalling. J. Exp. Bot. 2013, 64, 3099–3109.

Google Scholar: Author Only Title Only Author and Title

Zheng, X.Y., Spivey, N.W., Zeng, W., Liu, P.P., Fu, Z.Q., Klessig, D.F., He, S.Y., and Dong, X. (2012). Coronatine promotes Pseudomonas syringae virulence in plants by activating a signaling cascade that inhibits salicylic acid accumulation. Cell Host Microbe 11, 587–596.

Google Scholar: Author Only Title Only Author and Title

Spoel, S.H., and Dong, X. (2008). Making sense of hormone crosstalk during plant immune responses. Cell Host Microbe 3, 348–351.

Google Scholar: Author Only Title Only Author and Title

Laurie-Berry, N., Joardar, V., Street, I.H., and Kunkel, B.N. (2006). The Arabidopsis thaliana JASMONATE INSENSITIVE 1 gene is required for suppression of salicylic acid-dependent defenses during infection by Pseudomonas syringae. Mol. Plant Microbe Interact. 19, 789–800.

Google Scholar: Author Only Title Only Author and Title

Laudert, D., and Weiler, E.W. (1998). Allene oxide synthase: a major control point in Arabidopsis thaliana octadecanoid signalling. Plant J. 15, 675–684.

Google Scholar: Author Only Title Only Author and Title

Spoel, S.H., Koornneef, A., Claessens, S.M., Korzelius, J.P., Van Pelt, J.A., Mueller, M.J., Buchala, A.J., Me´traux, J.P., Brown, R., Kazan, K., et al. (2003). NPR1 modulates cross-talk between salicylate- and jasmonatedependent defense pathways through a novel function in the cytosol. Plant Cell 15, 760–770.

Google Scholar: Author Only Title Only Author and Title

Van der Does, D., Leon-Reyes, A., Koornneef, A., Van Verk, M.C., Rodenburg, N., Pauwels, L., Goossens, A., Ko¨ rbes, A.P., Memelink, J., Ritsema, T., et al. (2013). Salicylic acid suppresses jasmonic acid signaling downstream of SCFCOI1-JAZ by targeting GCC promoter motifs via transcription factor ORA59. Plant Cell 25, 744–761.

Google Scholar: Author Only Title Only Author and Title

Hong-Mei Yuan,Wen-Cheng Liu,Ying-Tang Lu. CATALASE2 Coordinates SA-Mediated Repression of Both Auxin Accumulation and JA Biosynthesis in Plant Defenses[J]. Cell Host & Microbe,2017,21(2).

Acknowledgments: This research was supported by the National Natural Science Foundation of China (31270655). We thank Meiqin Liu (Analysis and Testing Center, Beijing Forestry University) for her guidance on laser scanning confocal microscopy; Prof. Daoxin Xie (Tsinghua-Peking Joint Center for Life Sciences and MOE Key Laboratory of Bioinformatics, School of Life Sciences, Tsinghua University) for providing the plasmids: Cluc, Nluc pGreenII 0800-LUC and pGreenII 62-SK. All authors have approved the manuscript for publication, and no conflicts of interest exist.

Author Contributions: Design of research: J.G.and Y.S.Performed experiments: J.G., Z. G. and Z. W. L.Y. Analysed data: J.G., S. M., C.Z., S.L.Wrote the manuscript: J.G. All authors have read and agreed to the published version of the manuscript. J.G., Z.G. and Z.W. contributed equally to this work.

Conflicts of Interest: The authors declare no conflicts of interest.